(19) Europäisches Patentamt
European Patent Office
Office européen des brevets

(11) **EP 1 978 867 B1**

(12) **EUROPEAN PATENT SPECIFICATION**

(45) Date of publication and mention of the grant of the patent:
25.05.2011 Bulletin 2011/21

(21) Application number: **07823884.7**

(22) Date of filing: **05.06.2007**

(51) Int Cl.:
A61B 5/00 *(2006.01)* ***G01N 33/483*** *(2006.01)*
G01N 33/58 *(2006.01)*

(86) International application number:
PCT/GB2007/002067

(87) International publication number:
WO 2008/001037 (03.01.2008 Gazette 2008/01)

(54) METHODS FOR CHARACTERIZING TISSUES

VERFAHREN ZUR KENNZEICHNUNG VON GEWEBEN

PROCÉDÉS DE CARACTÉRISATION DE TISSUS

(84) Designated Contracting States:
AT BE BG CH CY CZ DE DK EE ES FI FR GB GR HU IE IS IT LI LT LU LV MC MT NL PL PT RO SE SI SK TR

(30) Priority: **05.06.2006 US 810930 P**

(43) Date of publication of application:
15.10.2008 Bulletin 2008/42

(73) Proprietor: **Forth Photonics Limited**
London EC2Y 5AB (GB)

(72) Inventor: **BALAS, Konstantinos**
GR-153 41 Athens (GR)

(74) Representative: **Spencer, Matthew Peter**
Boult Wade Tennant
Verulam Gardens
70 Gray's Inn Road
London WC1X 8BT (GB)

(56) References cited:
WO-A-01/72214 **WO-A-03/077750**
WO-A2-2004/005885 **US-A- 2002 007 122**

- **STEFANAKI I.M. ET AL: "In vivo detection of human papilloma virus-induced lesions of anogenital area after application of acetic acid: a novel and accurate approach to a trivial method" JOURNAL OF PHOTOCHEMISTRY AND PHOTOBIOLOGY B: BIOLOGY, vol. 65, no. 2-3, 31 December 2001 (2001-12-31), pages 115-121, XP007907524**

EP 1 978 867 B1

Description

FIELD OF THE INVENTION

[0001] The invention relates to methods for characterizing tissues and to automated and semi-automated diagnostic methods for *in vivo* screening, and for clinical diagnosis, respectively. The methods rely on the quantitative assessment of dynamic optical phenomena occurring in tissues after the application of specific biomarkers and on the determination of the predictive values of dynamic optical parameters.

BACKGROUND OF THE INVENTION

[0002] The existing diagnostic and screening procedures for detecting and grading epithelial cancers and pre-cancers are qualitative, subjective, multi-step, labour intensive and overall they are characterized by low cost effectiveness.

[0003] In the case of the cervix of the uterus the development of screening programs for cancer prevention targets the early detection and identification of its curable precursors such as Cervical Intraepithelial Neoplasia (CIN).

[0004] The Pap-test is the primary screening method for cervical neoplasia. During this test, a large number of cells are obtained from the cervical epithelium, and are cytologically examined after appropriate fixation and staining. The accuracy of this method is limited by both sampling and reading errors, leading to a significant false negative rate. A great number of studies have been performed aiming to determine the performance of the Pap-test over the past years. Researchers agree that the mean sensitivity is 0.59 and the mean specificity is 0.69-0.75 [Nanda K et al. (2000) Annals of Internal Medicine, 16;132(10): 810-819; Sankaranarayanana R, et al. (2005) International Journal of Gynecology and Obstetrics, 89:S4-S12; and Fahey MT et al. (1995) American Journal of Epidemiology, 141: 680-689]. It is also widely accepted that the Pap-test is unable to achieve concurrently high specificity and sensitivity. For example, a possible increase of specificity in the 0.90-0.95 range will result in a decrease of sensitivity in the 0.20-0.35 range [Fahey MT et al. (1995) American Journal of Epidemiology, 141: 680-689].

[0005] Typically, sensitivity (SS) and specificity (SP) are used as quantitative statistical parameters to describe the performance of diagnostic tests. The sensitivity expresses the percentage of the True Positives (TP), while specificity expresses the percentage of the True Negatives (TN). For example, a sensitivity of 80% (or 0.80) means that the test diagnoses correctly 80 of the 100 cases diagnosed as positive for the disease, with the aid of the gold standard test.

[0006] In a routine clinical setting, an abnormal Pap stained smear is followed by colposcopy, which involves examination of the cervix using a low power microscope. The cervical tissue is evaluated according to the following criteria: a) the morphology of the lesion's margins; b) the vascular pattern of abnormal epithelium; and c) the degree of staining after topical application of a marker, such as an acetic acid solution. Colposcopic grading is based solidly on visual examination, and the detected lesions are classified according to empirically qualitative scales. Clinical diagnosis based on the visual assessment (colposcopy) features a sensitivity of 0.77 and a specificity of 0.64 [Mitchell MF, et al. (1998) Obstetrics & Gynecology, 91:626-631]. Conventional colposcopy fails to diagnose 56% of microinvasive and 30% of invasive cervical cancer, leading to an inability to treat the lesion at its curable state. In addition, there is a high disagreement (77%) between two different physicians in identifying the most atypical site for biopsy. Researchers have reported a considerable inter-observer variability in identifying cervical lesions through colposcopy [Schiffman M, et al. (2003) Arch. Pathol. Lab. Med., 127: 946-949; NHS Report. Cervical Screening Programme, England: 2003-04 Statistical Bulletin 2004/20. October 2004. U.K; and Cantor SB, et al. (1998) Obstetrics & Gynecology, 91;(2): 270-277]. This diminishes the reproducibility of colposcopy and it is mainly attributed to the fact that the colposcopic assessment is qualitative and subjective.

[0007] In order to obtain more accurate CIN diagnosis and grading, biopsy samples are obtained from suspicious areas, which are then submitted for histological examination. Biopsy sampling poses several problems though, such as: a) subjectivity and high inter-observer disagreement (>30%), as revealed by the studies of Ismail *et al.* [Ismail SM, et al. (1989) British Medical Journal, 298;(6675): 707-710] Bellina *et al.* [Bellina JH, et al. (1982) South Med. J., 75;(1): 6-8. 56] and Robertson *et al.* [Robertson AJ, et al. (1989) J. Clin. Pathol., 42;(3): 231-238], and b) risks of sampling errors in selecting an abnormal site for biopsy.

[0008] The existing diagnostic chain for cervical neoplasia has reduced the incidence and mortality to historically low levels but further substantial reduction seems unlikely with the existing diagnostic procedures. This fact highlights the need for alternative, more efficient technologies, implementing the stand alone, and single step "see and treat" concept.

[0009] Over the last decade there has been a considerable effort towards the development of novel optical technologies capable of providing improved and objective information for the tissue pathology. These approaches are usually based on the fact that a tissue change from a normal to pathologic condition alters the tissue's structure and functionality, and also these alterations can be detected *in vivo,* by exploiting the light-tissue interaction phenomena. The measurement and analysis of the characteristics of the remitted light from the tissue can also provide information about the presence of different molecules, or about the various structural and functional changes occurring during the progress of the disease,

thus providing a means for the *in vivo* identification and grading of the lesion.

[0010] Previous attempts towards this direction include a variety of spectroscopic and spectral imaging techniques targeting the detection of biochemical and/or structural alterations *in vivo.* Indicatively, U.S. Pat. No 4,930,516 discloses a method for detecting cancerous tissue, where a tissue sample is illuminated with excitation light at a first wavelength, producing a fluorescent radiation in response to the excitation light detected. The discrimination between a cancerous vs normal tissue is based on the wavelength and amplitude of the emitted fluorescent radiation. Alternatively, the spectral amplitude of normal tissue will differ from that of a cancerous tissue at the same wavelength.

[0011] It is known that time resolved spectroscopy, which is based on monitoring the fluorescent decay time, has also a potential in discriminating the type, or condition, of an illuminated tissue. For example, U.S. Pat. No 5,562,100 discloses a method for determining tissue characteristics based on illuminating a target tissue with a short pulse of excitation radiation at a particular wavelength, and detecting fluorescent radiation emitted by the target tissue in response to the excitation. Tissue characteristics are determined from the recorded amplitude of the emitted radiation. In a similar manner, U.S. Pat. No 5,467,767 discloses a method for determining the malignant condition of a tissue, using time-resolved fluorescence spectroscopy.

[0012] Other inventions focus on combining two or more measurement techniques to determine tissue characteristics. For instance, U.S. Pat. No 6,975,899 discloses an apparatus and method utilizing fluorescence in combination with reflectance in order to de-couple the biochemical changes from the morphological changes occurring in a cancerous tissue. This combined approach is based on the fact that as tissue undergoes changes from a normal to a cancerous condition, fluorescence spectroscopy becomes less effective in determining tissue characteristics, as compared to absorption spectroscopy.

[0013] Other patents, such as U.S. Pat. No 5,369,496 to Utzinger et al., disclose a method and apparatus for diagnostic multispectral digital imaging using fluorescence, reflectance, and polarized reflectance spectroscopy. In U.S. Pat. No 6,427,082 a method and a system is provided for discriminating healthy from pathologic cervical tissue based on the fluorescence response of the tissue to laser excitation (LIF), and the back-scattered response to illumination by white light.

[0014] In general, prior art spectroscopic methods focus on tissue characteristics at a limited number of points on the tissue, whereas optical imaging methods focus on time-independent measurements of optical parameters over the entire tissue area. Moreover, these methods provide information only for the altered biochemical or cellular tissue structure, and not for the altered functionality of the epithelium.

[0015] Another approach developed by C. Balas is substantially different to the previous inventions since it involves measuring quantitatively the dynamic phenomena occurring in tissues after the application of biomarkers (PCT Publication No. WO 01/72214 A1 [Balas C. (2001) IEEE Trans. on Biomedical Engineering, 48:96-104], and [Balas CJ, et al. (1999) SPIE 3568: 31-37]). The measurement of the dynamic phenomena could potentially provide information for both structural and functional features of the tissue, facilitating an *in vivo* diagnosis.

[0016] The method and device disclosed therein relies on the administration of a pathology differentiating agent (biomarker), which has the property of enhancing the visualization of the altered structure and functionality of the abnormal cells selectively, and then it measures at any spatial point and in various wavelength bands, the remitted light as a function of time. The recorded intensity of the remitted light (for example intensity of back-scattered light (IBSL), defuse reflectance (DR) and fluorescence intensity), as a function of time is defined as the 'Dynamic Optical Curve' (DOC), which expresses the temporal characteristics of the optical phenomena generated during the tissue-biomarker interaction. Modeling and analysis of the acquired DOC enables calculation of a variety of Dynamic Optical Parameters (DOPs) characterizing the biomarker-tissue interaction kinetics at every image location (pixel or group of pixels). The spatial distribution of these parameters comprises the kinetic map, which can be overlaid onto the colour image of the tissue. These data could potentially provide a means for the *in vivo* detection, mapping and grading of the lesion for diagnosis, screening, and follow up, while simultaneously enabling guidance for biopsy sampling, and surgical treatment.

[0017] Typically, the clinical value of such a diagnostic technique is determined by its performance both in terms of its sensitivity (SS) and specificity (SP) positive and negative predictive value. If the SS and SP are greater than those of the existing diagnostic methods, then this new technology could be deemed suitable for screening or/and clinical diagnosis purposes.

[0018] US 2002/0007122 describes methods and systems for diagnosing disease in a sample by monitoring optical signals produced by samples in response to chemical agents.

[0019] Stefanaki et al (Journal of Photochemistry and Photobiology B: Biology 65 (2001) 115-121) relates to a method for staging of lesions and detection of HPV or neoplasia in a tissue.

[0020] Orfanoudaki et al (Gynecologic Oncology 96 (2005) 119-131) discuss quantitative methods to identify changes in the spectral properties of a tissue in response to chemical treatment, where the changes may be indicative of tissue abnormality.

[0021] WO 2004/005885 describes methods for determining a characteristic of a tissue sample, such as a state of health, using spectral data and/or images obtained within a period of time following the application of a chemical agent to the tissue sample.

SUMMARY OF THE INVENTION

[0022] The invention described herein provides improved methods as compared to the methods disclosed in PCT Publication No. WO 01/72214 A1; Balas C. (2001) IEEE Trans. on Biomedical Engineering, 48:96-104; and Balas CJ, et al. (1999) SPIE 3568: 31-37. Specifically, the present invention provides methods for automated diagnosis for screening purposes, or for semi-automated clinical diagnosis in colposcopy, based on selecting appropriate DOPs, along with their corresponding cut-off values, that best discriminate various pathologic conditions. This is achieved via correlation of the DOPs, extracted from the DOC, with both qualitative and quantitative pathology. The invention disclosed herein also provides methods for assessing both structural and functional features in a living tissue via modelling of epithelial transport phenomena, and their correlation with *in vivo* measured dynamic optical characteristics.

The present invention provides methods *e.g.*, automated or semi-automated methods, for characterizing (*e.g.*, grading) a tissue, such as, for example, a cancerous or pre-cancerous tissue (*e.g.*, of a cervical, uterine, oral, skin, respiratory, and gastrointestinal cancerous and/or pre-cancerous tissue).

[0023] The methods of the present invention are useful in, for example, facilitating the screening, clinical diagnosis, guided biopsy sampling or treatment of a tissue. The tissue may be an epithelial pre-cancer tissue or a cervical, uterine, oral, skin, respiratory or gastrointestinal pre-cancerous or cancerous tissue. The methods include plotting a dynamic optical curve based on the intensity of backscattered light from a tissue, or portion thereof, that has been exposed to a biomarker over time; based on the dynamic optical curve, determining a dynamic optical parameter, *e.g.*, 'Integral' or 'Max', based on the value of one or more of the dynamic optical parameters or sub-combinations thereof, characterizing the tissue. The dynamic optical curve represents the temporal variation of the intensity of the back-scattered light obtained from a tissue site after application of a biomarker and the dynamic optical parameter may be derived via a mathematical analysis of one or more of the dynamic optical curves or via empirical, manual, or visual analysis of one or more of the dynamic optical curves.

[0024] In a particularly preferred embodiment, the tissue under test is a cervical tissue. The methods are used to determine the nuclear to cytoplasmic ratio of the cells of the tissue. The tissue under test preferably comprises epithelial cells.

[0025] The methods of the invention preferably give at least 60% sensitivity and at least 60% specificity, even more preferably at least 65% or 70% sensitivity and at least 65% or 70% specificity and most preferably at least 75%, 76%, 77%, 78%, 79% or 80% sensitivity and at least 75%, 76%, 77%, 78%, 79% or 80% specificity.

In one embodiment, the biomarker is selected from a solution of acetic acid (*e.g.*, a 3-5% acetic acid solution), formic acid, propionic acid, butyric acid, Lugol's iodine, Shiller's iodine, methylene blue, toluidine blue, osmotic agents, ionic agents, and indigo carmine.

[0026] In another aspect, the present invention provides methods for characterizing the nuclear to cytopasmic ratio of a cervical tissue, such as a cervical cancer, or a pre-cancer tissue by plotting a dynamic optical curve based on an optical property observed from an imaged cervical tissue (for example the intensity of backscattered light from a cervical cancer or pre-cancer tissue) or portion thereof, that has been exposed to a biomarker over time; based on the dynamic optical curve, determining a dynamic optical parameter selected from the group consisting of 'Integral' and 'Max', based on the value of one or more of the dynamic optical parameters or sub-combinations thereof characterizing the cervical cancer or pre-cancer tissue.

It is confirmed that all embodiments listed in respect of the various aspects of the invention apply *mutatis mutandis* to the other related aspects of the invention and are not repeated for reasons of conciseness.

[0027] In one embodiment, the dynamic optical parameter 'Integral' is used to obtain information for the functional and structural characteristics of the tissue. In another embodiment, the dynamic optical parameter is 'Max' and the functional and structural characteristics of the tissue is nuclear-to-cytoplasmic-ratio.

[0028] In a further embodiment, the mathematical formulas correlating the nuclear-to-cytoplasmic-ratio (NCR) with the 'Integral' and 'Max' parameters are:

$$NCR = \frac{1}{1349} \times Integral - 0.278$$

and

$$NCR = \frac{1}{181} \times Max - 0.309 .$$

In related aspects, the invention also provides a computer readable medium holding computer program instructions for determining structural and functional characteristics of a tissue, which when executed by a computing device causes the computing device to perform the steps of:

calculating from an optical property of a tissue, or portion thereof that has been exposed to a biomarker over time, a dynamic optical curve,
determining at least one dynamic optical parameter from the dynamic optical curve,
comparing the value of the at least one dynamic optical parameter with at least one reference value of the at least one dynamic optical parameter known to be linked to a structural or functional characteristic of the tissue; and
based on the comparison, providing an output regarding a structural or functional characteristic of the tissue, or portion thereof, characterized in that the structural or functional characteristic of the tissue is nuclear-to-cytoplasmic-ratio,

wherein the at least one dynamic optical parameter is integral or max.

[0029] All appropriate embodiments relating to the methods of the invention apply *mutatis mutandis* to the computer readable medium aspects of the invention and *vice versa.*

[0030] Other features and advantages of the invention will be apparent from the following detailed description and claims.

BRIEF DESCRIPTION OF THE DRAWINGS

[0031] Preferred embodiments of the invention will now be described with reference to the following drawings, and the claims. In the drawings, like reference numerals are used to refer to like elements throughout the various views.

FIG. 1 is an illustration of the flowchart of the diagnostic method disclosed herein.

FIG. 2 shows typical DOCs obtained from cervical tissue sites interacting with acetic acid, corresponding to Human Papiloma Virus (HPV) infections, as classified by histology.

FIG. 3 shows typical DOCs obtained from cervical tissue sites interacting with acetic acid, corresponding to inflammation, as classified by histology.

FIG. 4 shows typical DOCs obtained from cervical tissue sites interacting with acetic acid, corresponding to Cervical Intraepithelial Neoplasia I (CIN I), as classified by histology.

FIG. 5 shows typical DOCs obtained from cervical tissue sites interacting with acetic acid, corresponding to high-grade (HG) lesions (CIN II, III, micro invasive cancer), as classified by histology .

FIG. 6 illustrates the DOPs corresponding to a typical DOC, which may be used for diagnosing various pathological conditions of the tissue.

FIG. 7 illustrates the Receiver Operator Characteristics (ROC) curve corresponding to an indicative DOP (Integral) and the 'area under the ROC curve', expressing the performance of this particular DOP in discriminating low-from high-grade CIN. The results have been obtained from cervical epithelia *in vivo,* interacting with acetic acid solution, in a clinical setting where 310 women have been enrolled.

FIG. 8 shows the sensitivity (grey) and specificity (black) plots derived from ROC analysis corresponding to an indicative DOP (Integral), expressing the performance of this particular DOP in discriminating low-grade from high-grade lesions. Integral values selected from the range 480 to 650 comprise a cut-off value for discriminating Low from High Grade cervical neoplasias with both SS and SP being greater than 60%. The results have been obtained from cervical epithelia *in vivo,* interacting with acetic acid solution 3%, in a clinical setting where 310 women have been enrolled.

FIGS. 9A-E show the mean values, with corresponding error-bars, for five different DOPs extracted from the DOC. The results have been obtained from cervical epithelia *in vivo,* interacting with acetic acid solution, in a clinical setting where 310 women have been enrolled.

FIGS. 10A and 10B show scatter plots and linear regression curves of nuclear-to-cytoplasmic-ratio (NCR), assessed quantitatively in tissue samples against two different DOPs (Integral and Max) obtained from the same samples before biopsy. The results have been obtained from cervical epithelia *in vivo,* interacting with acetic acid solution, in a clinical setting where 310 women have been enrolled.

FIG. 11 shows typical DOCs obtained from cervical tissue sites interacting with acetic acid, corresponding to healthy (normal) tissue, as classified by histology.

FIG. 12 shows the steps followed by a software implementation of the invention disclosed herein in connection with an exemplary embodiment of the hardware setup utilized to acquire the image tissue data.

DETAILED DESCRIPTION OF PREFERRED EMBODIMENTS

[0032] Optical biomarkers are chemical substances that induce impermanent alterations of the optical response of the abnormal tissue. In the case of efficient biomarkers, the structural, morphological and functional alterations of the abnormal tissue are manifested in the optical signal generated during the biomarker tissue interaction facilitating lesion identification and localization:

A typical diagnostic procedure involving biomarker application includes:

- Administrating topically or systematically one or more biomarkers.
- Inspection of the biomarker induced alterations in the optical properties of the tissue.
- Locating abnormal areas for diagnosis and treatment.

Traditional diagnostic methods involving biomarkers suffer from several drawbacks mainly related to the fact that the visual assessment of dynamic optical phenomena cannot be effective, due to physiological limitations of the human optical system in detecting and recording fast changing phenomena with different kinetics in different tissue sites.

[0033] A solution to this problem is provided by a method and device disclosed by Balas C. (2001) IEEE Trans. on Biomedical Engineering, 48:96-104; Balas CJ, et al. (1999) SPIE 3568: 31-37; and PCT Publication No. WO 01/72214 A1, wherein quantitative assessment and mapping of the dynamic optical phenomena generated from the biomarker-tissue interaction is provided.

[0034] As indicated above, the present invention provides improved methods as compared to the foregoing methods. For example, the present invention provides a systematic parametric analysis of DOC and comparative evaluation of the derived DOPs in terms of both predictive value and efficiency in discriminating various normal and pathologic conditions.

[0035] The invention described herein pertains to methods for automated diagnosis for screening purposes, or for semi-automated clinical diagnosis in colposcopy, based on selecting appropriate DOPs, along with their corresponding cut-off values, that best discriminate various pathologic conditions. This is achieved via correlation of the DOPs, extracted from the DOC, with both qualitative and quantitative pathology. Another objective of the invention disclosed herein is to present a method for assessing both structural and functional features in a living tissue via modelling of epithelial transport phenomena, and their correlation with *in vivo* measured dynamic optical characteristics.

[0036] As used interchangeably herein, the terms "dynamic optical curve" or "DOC" are intended to include a curve representing an optical characteristic of a tissue under observation, such as intensity of backscattered light from a tissue or portion thereof, reflectance of light, diffusive reflectance of light from a tissue or a portion thereof, or fluorescence from a tissue or a portion thereof that has been exposed to a biomarker over time.

[0037] As used herein, the term "biomarker" is intended to include any chemical agent capable of altering an optical signal from the tissue sample being tested. Non-limiting examples of such agents include, but are not limited to acetic acid, formic acid, propionic acid, butyric acid, Lugol's iodine, Shiller's iodine, methylene blue, toluidine blue, osmotic agents, ionic agents, and indigo carmine. Any solutions of the foregoing agents may be used. In a preferred embodiment, the biomarker is an acetic acid solution, *e.g.*, a 3-5% acetic acid solution.

[0038] As used herein, the term "dynamic optical parameter" is intended to include the one or more parameters based on which one of skill in the art may characterize, *e.g.*, grade, a tissue. As described herein such parameters may be derived via a mathematical analysis of one or more of the dynamic optical curves plotted based on the intensity of backscattered light from a cancer tissue, or portion thereof, that has been exposed to a biomarker over time. Such parameters may also be derived by an empirical, manual, or visual analysis of one or more of said dynamic optical curves. The dynamic optical parameters contemplated by the present invention are 'Integral' and 'Max'.

[0039] Numerical values of these dynamic optical parameters are based upon those obtained with a digital imaging system (DySIS technology, Forth Photonics) calibrated against an 18% reflecting calibration specimen to produce for the latter a gray value of 105 in a 0-255 gray scale in the green channel of the system. Based on this calibration protocol Max is given as green gray value max difference in calibrated units (scale 0-255) or as reflectance max difference (scale 0-100%).

[0040] The integral cut-off values referred to herein have been calculated from a DOC corresponding to a τ=240 sec integration time:

$$Itg = c\int_{0}^{240}(I_t - I_{t=0})dt$$

[0041] Where c is a scaling factor with value c= $8[\tau I_{t=0}]^{-1}$ or by substituting c=1/30 (intensity units)$^{-1}$sec^{-1}, I, is the remitted intensity at a given time point after the application of the biomarker , and $I_{t=0}$ is the remitted intensity before the application of the biomarker.

[0042] Area to max is calculated from the same Itg formula and the only difference is that τ=Tmax. Accordingly, both Itg and Area-to-Max values are presented herein as dimensionless quantities.

[0043] Different acquisition, integration time periods and calibration protocols and samples may result in different cut-off values. The 240 sec integration time period is selected as an optimum time period and it is presented here as an example and not as a restriction. The "calibrated units" and "dimensionless quantities" disclosed herein may also be referred to as "arbitrary units".

[0044] Thus, the values referred to herein indicate those obtained via the specific protocol above. This provides the skilled person with a readily identifiable method for comparison of quantitative values obtained through use of other imaging systems.

[0045] The articles "a" and "an" are used herein to refer to one or to more than one (*i.e.* to at least one) of the grammatical object of the article. By way of example, "a dynamic optical parameter" means one or more dynamic optical parameters.

[0046] As used herein, the term "tissue" is intended to include any tissue, or portions thereof, including cancerous and pre-cancerous tissues. For example, the tissue may be an epithelial tissue, a connective tissue, a muscular tissue or a nervous tissue. In a preferred embodiment of the invention, the tissue is an epithelial tissue, or a portion thereof, *e.g.*, covering and lining epithelium or glandular epithelium. For example, the tissue may be cervical tissue; skin tissue; gastrointestinal tract tissue, *e.g.*, oral cavity tissue, stomach tissue, esophageal tissue, duodenal tissue, small intestine tissue, large intestine tissue, pancreatic tissue, liver tissue, gallbladder tissue or colon tissue; or nasal cavity tissue. In a preferred embodiment, the tissue is a pre-cancer or cancer tissue, such as, for example, a dysplasia, a neoplasia or a cancerous lesion.

[0047] As used herein, the phrase "characterizing" a cancer tissue is intended to include the characterization of a cancer tissue using the methods described herein such that the screening, clinical diagnosis, guided biopsy sampling and/or treatment of a cancer tissue is facilitated. For example, a cancer tissue may be graded, *e.g.*, characterized as a low grade (LG) lesion (*i.e.*, an HPV infection, an inflammation or a CIN Grade I lesion, or a sub-combination thereof) or a high grade (HG) lesion (*i.e.*, a CIN Grade II lesion, a CIN Grade III lesion, or Invasive Carcinoma (CA) or a sub-combination thereof).

[0048] As used herein, tissue characteristics include, but are not limited to, structural characteristics and functional characteristics of a tissue, as well as any combination of the aforementioned.

[0049] There are various degrees of cervical intraepithelial neoplasia (CIN), formerly called dysplasia. Histologically evaluated lesions are typically characterized using the CIN nomenclature; cytologic smears are typically classified according to the Bethesda system; and cervical cancer is typically staged based on the International Federation of Gynecology and Obstetrics (FIGO) system. CIN Grade I (mild dysplasia) is defined as the disordered growth of the lower third of the epithelial lining; CIN Grade II (moderate dysplasia) is defined as the abnormal maturation of two-thirds of the lining; CIN Grade III (severe dysplasia): encompasses more than two thirds of the epithelial thickness with carcinoma *in situ* (CIS) representing full-thickness dysmaturity. There are well known classification systems for the characterization of cervical dysplasia, *i.e.*, the disordered growth and development of the epithelial lining of the cervix (see, for example, DeCherney, A. et al., Current Obstetric & Gynecologic Diagnosis & Treatment, 9th ed., The McGraw-Hill Companies, New York, NY (2003).

[0050] "Reference values" relate to predictive and cut-off values of the various dynamic optical parameters (DOPs) which correlate with and can be used to discriminate specific structural and functional characteristics of a tissue.

[0051] **FIG. 1** illustrates the basic steps of the method of the invention.

- Acquisition of a reference image of the tissue before biomarker application, **102.** This step is required in order to record the original optical properties of the examined tissue.
- Application of a biomarker, *e.g.*, by means of an applicator, **104.** The biomarker applicator may also provide a triggering signal to initiate image acquisition, right after (i.e., less than 1 second) the biomarker application, thus ensuring the synchronization and the standardization of the acquisition process.
- Acquisition of a series of images in time succession at a sampling or acquisition rate of between about five and seven seconds, at predetermined spectral bands, and for a predetermined time period of about four minutes, 106. The time period is determined taking into account the duration of the optical phenomena induced by the biomarker.

Those skilled in the art will recognize that the time period can extend beyond four minutes to one or two hours or any time interval therebetween, but factors such as patient comfort, patient convenience, effectiveness of optical phenomena induced by the biomarker beyond a certain period, system capabilities such as storage capacity and processing capacity, and other like factors can be used to determine a desired time period. Alternatively, the time period can be measured in terms of the number of images acquired, for example, thirty images, thirty-five images, forty images and the like. Spectral bands are selected such that maximum contrast between biomarker responsive and non responsive areas is achieved.

• Align captured images, 108. This step is essential for obtaining the temporal variation of light intensity emitted by every tissue point. Image pixels corresponding to a specific image location need to correspond to the same tissue point. In several cases of *in vivo* measurements, the optical sensor-tissue relative movements are present due to breathing, etc, during successive acquisition of tissue images. Constant relative position between the optical sensor and the examined tissue area may be ensured, for example, through either mechanical stabilization means, and/or image registration algorithms. Proper alignment of the captured images with the reference image **(102)** ensures also valid extraction of the DOC from every image pixel or group of pixels corresponding to a specific location of the examined tissue.

• Calculation from some or all of said acquired series of images of the DOC at every image location (i.e., every pixel location or a location defined by a group of pixels) for selected images, expressing the diffuse reflectance [DR], or fluorescence intensity (FI), as a function of time at predetermined spectral bands, 110. The selection of the optical property (DR, FI) is determined by the property of the employed biomarker to alter either the diffuse reflectance, or fluorescence characteristics, respectively. As indicated above, proper spectral bands are selected providing the maximum contrast between biomarker responsive and non-responsive tissues and tissue areas. In an illustrative embodiment, **FIG. 2-5** to be described below, show DOC curves obtained from cervical tissue sites interacting with acetic acid solution (biomarker) corresponding to various pathologies, as classified by histology.

• Calculation of DOPs from DOC obtained from each image location (i.e., every pixel location or a location defined by a group of pixels) for selected images, **112.** A number of parameters expressing the dynamic characteristics of the phenomenon are derived. Depending on the efficiency of the biomarker in selectively staining tissue abnormalities, DOPs could potentially provide a quantitative means for assessing *in vivo* various tissue pathologies. These parameters can then be displayed in the form of a pseudocolor map, with different colors representing different parameter values. Such a pseudocolor map can be used for determining the lesion's grade and margins, thus facilitating biopsy sampling, treatment, and in general lesion management. In one embodiment of the current invention, a variety of DOPs are calculated from DOC (*e.g.*, DOC integral over selected time ranges, maxima, slopes as indicated in, for example, Table 1 below) expressing the dynamic characteristics of the optical phenomena generated by biomarker-tissue interaction. Detailed analysis of indicative DOPs is provided below for the case where the tissue is cervical epithelium and the biomarker is an acetic acid solution with reference to FIG. 6.

• In another embodiment the predictive value of the DOPs and DOC is determined experimentally in a statistically sufficient tissue population by comparing DOP and DOC vales with standard methods providing definite diagnosis, such as histology (gold standards). For those DOPs displaying adequate predictive values, cut-off values that best discriminate various pathological conditions are determined, 116. For a specific biomarker and epithelial tissue this step could be performed separately and not as a part of the routine implementation of the method. This step is essential for correlating DOPs and DOC with specific pathological conditions. After establishing this correlation discrimination of pathological conditions based on predetermined cut-off values of DOPs is enabled 120. Detailed analysis of the assessment of the predictive values of various DOPs in the case where the tissue is cervical epithelium and the biomarker is acetic acid solution is provided below with reference to **FIGS. 7-9.**

• DOP and DOC values representing different pathological conditions and grades can be displayed in a form of a pseudocolor map, wherein different colors represent different grades, **124.** The pseudocolor map expresses a pathology map which can be used for the *in vivo* grading of the lesion, and the determination of the lesion margins, facilitating biopsy sampling, treatment and in general the management of the lesion.

• In another embodiment of the current invention, biophysical models of both transport phenomena and structural features of an epithelial tissue are developed based on the understanding and the analysis of biomarker-tissue interaction through *in vivo* and *in vitro* experiments, **114.** In cases where epithelial transport phenomena are determined by the functional characteristics of the tissue, and in cases where the functional characteristics are expressed in DOPs and DOC, the model parameters are correlated with the later, thus providing a means for the *in vivo* assessment of functional and structural characteristics of the tissue. In particular, DOP values may be converted to express functional and/or structural features of the tissue in various normal and pathological conditions, **118.** It is worth noticing that functional properties can be determined only in living tissues, whereas structural features can be determined *in vitro* by analyzing tissue samples (biopsies). The methods of the present invention provide a means for assessing both features *in vivo,* thus, enabling more complete epithelial system characterization or identification. Complete epithelial system characterization/identification is expected to improve diagnostic perform-

ance since various pathological conditions affect both functional and structural properties of an epithelial tissue. As an example, and referring to structural phenomena for the case of cervical cancer where acetic-acid solution is used as a biomarker, DOP values are correlated with quantitative data expressing nuclear density obtained through quantitative pathology methods. The correlation is illustrated in **FIG. 10-11,** which enables the conversion of DOP to nuclear-to-cytoplasmic-ratio. In both cases of either functional or structural features, a pseudocolor map may be generated with different colors representing different functional and structural features, **122.** The pseudocolor map expresses either a tissue functionality and/or structural map, which can be used for the *in vivo* grading of the lesion, and the determination of the lesion margins, facilitating biopsy sampling, treatment and in general management of the lesion. The pseudocolor map may be also used for *in vivo* monitoring of the effects of the biomarker in both structural and functional features of the tissue and, consequently, for assessing the efficiency of the biomarker in highlighting abnormal tissue areas.

[0052] As an illustrative embodiment of the present invention in the case of cervical tissue, the appropriate DOPs, and corresponding cut-off values were determined that best discriminate among conditions including normal, HPV (Human Papillomavirus) infection, Inflammation, and Cervical Intraepithelial Neoplasia (CIN) of different grades. Acetic acid solution 3-5% was used as the biomarker and the above mentioned measuring procedure for obtaining the DOC was followed. In order to determine the predictive value of DOC and DOPs, experimental data were obtained from a multi-site clinical trial, where 308 women with abnormal Pap-test were enrolled and examined. DOCs were obtained though image capturing in time sequence of the cervical tissue in the blue-green spectral range. The acetic acid responsive tissue areas, as depicted by a DOC and DOPs pseudocolor map, were biopsied and submitted for histological evaluation and grading. The histology classification was then compared with a set of DOPs in order to determine those that best correlate with histology grading through ROC analysis. From the ROC curve, the optimum cut-off values for each parameter, or for a set of parameters, were derived providing the desirable SS and SP values.

[0053] In an illustrative embodiment, **FIG. 2** to **FIG. 5** show typical DOC obtained from cervical tissue sites classified by the histologists as: HPV infection, Inflammation, CIN1, and high-grade (HG) lesions, respectively. As a further categorisation used commonly in clinical practice, HPV, Inflammation, CIN1, or combination thereof, are referred to as low-grade (LG) lesions. HG lesions correspond to either, or combination of, CIN2, CIN3, or Invasive Carcinoma (CA). Histological grades CIN1, CIN2, and CIN3 are precursors of CA (CIN1-lowest, CIN3-highest). The vertical axis corresponds to the IBSL (expressed in arbitrary units), and the horizontal axis represents the elapsed time (in seconds) after the application of acetic acid to the tissue. It is clearly seen that the DOC corresponding to the various pathologic conditions differ in various ways in terms of intensity-temporal alterations.

[0054] In particular, it can be seen that the HPV-classified curves increase almost exponentially and then reach a saturation level, whereas the curves corresponding to inflammation reach a higher peak value earlier, and then decay abruptly. CIN1-classified curves reach their maximum later than the curves corresponding to HPV or inflammation, and then decay with a slow rate, that is notably slower than that observed in the inflammation cases. For the HG lesions, the maximum of the curves is reached later and with a higher value than that observed in the HPV and CIN1 cases, whereas the decay rate is very small; much smaller than that seen in the inflammation-classified curves. In contrast to these findings, the DOC obtained from a normal tissue site are almost constant across the entire measurement period (see **FIG 11).**

[0055] Although helpful, the previous description of the DOC in relation to a specific pathological condition is rather qualitative. Hence, the following sections describe the quantitative parameters extracted from the dynamic curves which are able to discriminate robustly LG from HG lesions, and HPV infections from HG lesions.

[0056] In a preferred embodiment of the invention, the DOC obtained from the tissue can be further processed using mathematical formulations, including, but not limited to, polynomial, single-, bi-, and multi-exponential fitting, linear and non-linear decomposition, or combinations thereof, in order to derive a single, or combination of, DOPs depicting various characteristics of the recorded DOC in relation to a pathological condition.

[0057] In another embodiment, the derived DOPs can be also weighted based on features particular to the examined tissue sample, such as, for example, patient age, menopausal period (for women), or on features characterizing the regional, global, population of the subject whose tissue is examined, or both.

[0058] The DOPs with a high diagnostic value in discriminating LG from HG lesions are the following:

1. Max

[0059] This parameter is defined as the difference between maximum value of the recorded DOC, after the application of a biomarker and DOC value at t=0

2. Integral

[0060] This parameter is defined as the area surrounded by the recorded DOC, and the parallel to the time axis line intersecting the first DOC experimental point. The integral is calculated for a predetermined time period, which depends on the time duration of optical effects generated by the biomarker-tissue interaction. In the case of cervical tissue and acetic acid solution (biomarker) the integral is taken for t=0 to t=4 min. This parameter can be also calculated analytically through the integral of a mathematical formula, after approximation of the measured curve with a closed mathematical form.

3. Tmax

[0061] This parameter is defined as the time required for reaching the maximum of the DOC, where said maximum is the Max parameter.

4. Area to Max

[0062] This parameter is defined as the area of the curve corresponding to the DOC from t = 0 sec (i.e., initialization time of the acetowhitening phenomenon), until t = *Tmax*. Again, this parameter can also be calculated analytically through the integral of a mathematical formula, after approximation of the measured curve with a closed mathematical form.

5. SlopeA

[0063] This is a parameter expressing the rate of intensity increase until the 'Max' value. Indicatively, it can be calculated as the first derivative of the curve, or as the average of the intermediate slopes until the 'Max' value is reached.

6. SlopeB

[0064] This is a parameter expressing the rate of intensity decrease starting from the 'Max' value of the curve. Indicatively, it can be calculated as the last derivative of the curve, or as the average of the intermediate slopes, starting from the 'Max' value.

[0065] **FIG. 6** illustrates four of the previously defined parameters on the curve of a DOC: 'Max', 'Tmax', 'SlopeA', and 'SlopeB'. The other two parameters ('integral', and 'Area to Max'), represent essentially the area enclosed by the indicated points: *KLNP,* and *KLM*, respectively.

[0066] **FIG. 7** illustrates the LG/HG ROC analysis of the cumulative results for the 'Integral' parameter described previously. The area under the ROC curve is 0.83, implying high discrimination (sensitivity).

[0067] **FIG. 8** illustrates the sensitivity (grey) and specificity (black) plots derived from the ROC analysis for various values of the 'Integral' parameter used for the quantification of the acetowhitening characteristics. It is clearly seen that for a certain value both sensitivity and specificity are maximized reaching 78%.

[0068] **FIG. 9** illustrates the mean values, with corresponding error-bars representing 95% confidence intervals, for some of the parameters described previously, for the LG and HG diagnostic conditions, as concluded through biopsy examination performed by the histologists.

[0069] The optimum value ranges in discriminating LG from HG lesions were calculated with ROC analysis, as shown previously for the 'Integral' parameter. In particular, for each parameter type the percentage of true positives (TP) and false positives (FP) was calculated for various threshold values spanning the entire range: [Pmin, Pmax], where P denotes the value of a specific parameter. The threshold value where the sensitivity (SS = TP), and specificity (SP = 100-FP), approximately coincide with one another was used as an optimum (cut-off) value for discriminating LG from HG.

[0070] **TABLE 1** illustrates the optimum value ranges for discriminating LG from HG lesions for some of the previously defined parameters, leading to a performance dictated by specificity and sensitivity greater than 60%.

TABLE 1

Parameter	Optimum parameter cut-off values for LG/HG discrimination
Max*	70 to 90 (calibrated units) or 15-25% (reflectance)
Integral**	480 to 650 (dimensionless quantity)
Tmax	80-100 sec
Area to Max**	120 to 170 (dimensionless quantity)

(continued)

Parameter	Optimum parameter cut-off values for LG/HG discrimination
SlopeA	1.1 to 1.3 (rad)
SlopeB	-0.012 to -0.090 (rad)

*The parameters listed above have been obtained with a digital imaging system (DySIS technology, Forth Photonics) calibrated against an 18% reflecting calibration specimen to produce for the later a gray value of 105 in a 0-255 gray scale in the green channel of the system. Based on this calibration protocol Max is given as green gray value max difference in calibrated units (scale 0-255) or as reflectance max difference (scale 0-100%)

**The presented integral cut-off values have been calculated from a DOC corresponding to a τ=240 sec integration time:

$$Itg = c \int_0^{240} (I_t - I_{t=0})dt$$

[0071] Where c is a scaling factor with value c= $8[\tau I_{t=0}]^{-1}$ or by substituting c=1/30 (intensity units)$^{-1}$sec^{-1}, I_t the remitted intensity at a given time point after the application of the biomarker, and $I_{t=0}$ the remitted intensity before the application of the biomarker.

[0072] Accordingly, Area to max is calculated from the same Itg formula and the only difference is that τ=Tmax. Both Itg and Area-to-Max are presented here as dimensionless quantities.

[0073] Different acquisition, integration time periods and calibration protocols and samples may result in different cut-off values. The 240 sec integration time period is selected as an optimum time period and it is presented here as an example and not as a restriction.

[0074] **TABLE 2** illustrates the optimum value ranges generating specificity and sensitivity greater than 60% for HPV/HG discrimination, for the 'Max' and 'Integral' parameters.

TABLE 2

Parameter	Optimum parameter cut-off values for HPV/HG discrimination
Max	65 to 90 (calibrated units)
Integral	380 to 490 (dimensionless quantity)

[0075] Combinations of parameters including but not limited to the above mentioned may provide a means for determining the pathology of tissue. For example, such a parameter may be the product of the average slope DOC until about 40 sec sampling time after the application of said biomarker, by the Max value. Product values greater than about 2.05 ± 0.2 (calibrated intensity units/time) may indicate the presence of high grade neoplasia, whereas lower values may indicate low grade neoplasia or healthy tissue.

[0076] Beyond the 'hard-clustering' approach using a cut-off parameter value for discriminating LG from HG lesions, or HPV from HG lesions, more advanced statistical and pattern recognition analysis techniques (such as Bayesian classification, Artificial Neural Networks (ANNs), classification trees), may be employed to extract other linear, or non-linear, of single or combinations of multiple, parameters for achieving high discrimination. A parametric approach, using Bayesian modelling (as described in, for example, Fukunaga K. (1990) *New York: Academic,* 2nd Ed.), and a non-parametric approach, using ANNs (Learning Vector Quantization-LVQ, see as described in, for example, Kohonen T., (1986) Int. J. Quant. Chem., Suppl. 13, 209-21), were employed for differentiating the DOPs obtained from corresponding DOC of tissue sites with LG and HG neoplasia. For both Bayes and NN classification, the overall discrimination performance of LG and HG lesions was greater than 75%, for various combinations of the optical parameters described previously, and for a variable number of training sets selected from the overall sample.

[0077] In another embodiment, the invention comprises a means for automated cervical screening through the mapping of the dynamic parameter values, and the corresponding cut-off values, showing presence of the disease.

[0078] In yet another embodiment, the invention comprises a means for semi-automated colposcopy through the mapping of the dynamic parameter values and corresponding cut-off values showing presence of the disease. Such a methodology ensures a base-line colposcopy performance independently of the practitioner's skills, facilitating the overall diagnostic procedure, follow-up, and guidance during biopsy sampling and treatment.

[0079] Another aspect of the present invention comprises the interpretation of the acetowhitening phenomenon dictated

by the dynamic parameters in relation to the functional and structural alterations in the epithelium. In one embodiment, distinctive parameters related to the cervical tissue structural properties are computed and correlated with a number of functional features derived from the DOC recorded from the same tissue sites. Specifically, there is a common agreement in terms of the direct correlation between the nuclear volume and grading of neoplasia (HPV, CIN 1, CIN 2 and CIN3), or cervical cancer [Walker DC, et al. (2003) Physiological Measurement, 24:1-15]. The nuclear-to-cytoplasmic-ratio (NCR), which expresses the nuclear density in the epithelial tissue, is the most common parameter used to describe this correlation with certain diagnostic conditions. In a preferred embodiment, the cellular structure of the tissue is assessed by finding the correlation formula between either, or combination, of the aforementioned dynamic parameters with the NCR computed from the biopsy material extracted from corresponding cervical locations. To this end, the NCR was correlated with the DOC parameters reflecting the abnormal functioning of the epithelium, after acetic acid induction into the tissue area.

[0080] In yet another embodiment, this correlation could lead to the extraction of a pseudocolor map representing the structural properties of the examined cervical tissue at every location, in addition to the map representing the acetowhitening kinetic characteristics, along with highlighted sites of high nuclear density. Such an implementation has an exceptional value if one thinks that by quantifying the *in vivo* optical curve obtained from the tissue, which represents an *in vivo* assessment of the macro-structural tissue state; one can also derive direct conclusions about the cellular properties of the tissue, which constitutes a representative view of its structure at a microscopic level.

[0081] In order to calculate the NCR for a corresponding number of epithelial tissue sites from which the dynamic parameters were obtained by the method disclosed herein, an equal number of cervical biopsy samples were obtained during colposcopy. The biopsied tissue was processed through standard procedures, immunohistochemically stained, and placed on slides for further evaluation through microscopic image analysis. After acquiring an equivalent number of microscopic histological images, a multistage image-analysis algorithm was employed for segmenting the cell-nuclei displayed in the images [Loukas CG, et al. (2003) Cytometry, 55A(1): 30-42]. The NCR quantity was calculated as the sum of the area occupied by the nuclei enclosed in the epithelium, divided by the overall area of the epithelial tissue. NCR is also known as the 'cell-packing' property of the epithelial tissue, expressing essentially the cross-sectional structure of the tissue's cellular population.

[0082] In an illustrative embodiment, **FIG. 10A** and **FIG. 10B** show scatter plots of two different DOPs exhibiting the strongest correlation coefficient (R), against NCR. These parameters are the 'Integral', and the maximum value (Max), of the dynamic optical curve, as defined previously. The lines in the graphs represent linear regression curves, whereas the DOP to NCR conversion equation and correlation results obtained from least-squares fitting on the experimental data are shown in **TABLE 3.**

TABLE 3

NCR *vs* DOP	Correlation Coefficient	Conversion Equation
NCR *vs* 'Integral'	0.71	$NCR = \frac{1}{1349} \times Integral - 0.278$
NCR *vs* 'Max'	0.64	$NCR = \frac{1}{181} \times Max - 0.309$

From this table it can be seen that both parameters present a significant correlation with the cell-packing property of the tissue. In one embodiment of the method, the linear equations allow conversion of a DOP corresponding to a DOC obtained from a specific tissue site, to the underlying NCR property of the tissue site.

[0083] In another embodiment of the method, either of the quantitative pseudocolor maps of 'Integral', or 'Max', can be converted to the NCR map of the epithelial tissue, using the previously shown conversion formulas.

[0084] In addition to the structural alterations of the epithelial tissue in relation to neoplasia progression, there are also several functional changes in the extracellular and intracellular space of the epithelium after applying the acetic acid solution. In particular, solid tumours are known to live in an acidic microenviroment [Webb SD, at al. (1999) J. Theor. Biol., 196: 237-250; Lee AH, et al. (1998) Cancer Research, 58: 1901-1908; Yamagata M et al. (1996) Br. J. Cancer, 73: 1328-1334; and Marion S, et al. (2000) Molecular Medicine Today, 6: 15-19]. Besides, experimental measurements have shown that extracellular pH in tumors is on average 0.5 units lower than that of normal tissues, with tumor extracellular pH lying typically in the range [6.6-7.0] (see [Yamagata M et al. (1996) Br. J. Cancer, 73: 1328-1334]). Tumor cells also have a neutral or slightly alkaline intracellular pH [Marion S, et al. (2000) Molecular Medicine Today, 6: 15-19]. Similar to the normal cells, tumor cells regulate their cytoplasmic pH within a narrow range to provide a favorable environment

for various intracellular activities.

[0085] Although the issue regarding the presence of acidic extracellular pH in tumors is still controversial, there is a common belief that the acidic environment of tumors arises from the high rate of metabolic acid production, such as lactic acid, and from its inefficient removal from the extracellular space [Webb SD, at al. (1999) J. Theor. Biol., 196: 237-250; Lee AH, et al. (1998) Cancer Research, 58: 1901-1908; Marion S, et al. (2000) Molecular Medicine Today, 6: 15-19; and Prescott DM, et al. (2000) Clinical Cancer Research, 6;(6): 2501-2505]. Besides, tumor cells have a high rate of glycolysis, regardless of their oxygen supply level. As a consequence, large quantities of lactic acid (and subsequently H^+) are produced outwards from the cellular environment. Due to a number of factors such as a disorganized vasculature, or poor lymphatic drainage, and elevated interstitial pressure, the acid clearance (H^+ clearance) to the blood is very slow, and thus a reversed pH gradient between the extracellular and the intracellular space of tumors cells is observed, [Webb SD, at al. (1999) J. Theor. Biol., 196: 237-250; Lee AH, et al. (1998) Cancer Research, 58: 1901-1908; Yamagata M et al. (1996) Br. J. Cancer, 73: 1328-1334; and Marion S, et al. (2000) Molecular Medicine Today, 6: 15-19]. It is also reasonable to assume that the CIN extracellular environment is also acidic (perhaps less acidic), provided that cancer is a transitional process and CIN is a precursor of cancer. Moreover, tumor as well as dysplastic cells are known to employ the same short-term, [Marion S, et al. (2000) Molecular Medicine Today, 6: 15-19], and long-term [Lee AH, et al. (1998) Cancer Research, 58: 1901-1908; Yamagata M et al. (1996) Br. J. Cancer, 73: 1328-1334 and Prescott DM, et al. (2000) Clinical Cancer Research, 6;(6): 2501-2505], pH regulation mechanisms as those of normal cells. The excess of protons produced by tumor cell metabolism is excreted from the cell via specific hydrogen pumps [Prescott DM, et al. (2000) Clinical Cancer Research, 6;(6): 2501-2505].

[0086] The observation of the acetowhitening effect in the cervix is used in colposcopy to characterize abnormal tissue (i.e. HPV, CIN, or cancer). The acetowhitening effect refers to the phenomenon induced by the application of acetic acid solution to the cervical transformation zone. The acetic acid application selectively induces a transient whitening of abnormal cervical areas. Although it has been used for more than 70 years in clinical practice to locate abnormal areas, the exact physicochemical mechanisms involved in tissue whitening remain still unknown. Similar phenomena are observed when Formic, Propionic, and Butyric, acids are employed as biomarkers.

[0087] Two major explanations for the interpretation of the acetowhitening effect prevail in the relative literature. *In vitro* studies have shown that the acetic acid effect is related to the amount of certain cytokeratines (proteins present in epithelial cells) [Maddox P, et al. (1999) Journal of Clinical Pathology, 52: 41-46 and Carrilho C, et al. (2004) Human Pathology, 35: 546 - 551]. Since in cervical neoplasias the extra-cellular environment is acidic, the topically administered acetic acid molecule is not disassociated to its composing ions and as such can penetrate passively the cell membrane. Entering into the neutral pH cytoplasm the acetic acid molecules are disassociated giving hydrogen and carboxylic ions which interact with nuclear proteins resulting in the alteration of the scattering properties of the abnormal cells selectively.

[0088] Cytosolic pH value is crucial for the conformational stability of these proteins. At neutral pH values, proteins are stable in solution. As pH drops, they become unstable and insoluble depending on their pI (isoelectrical point). The process of protein destabilization is called denaturation and this partial denaturation is a reversible process which lasts only for some milliseconds. Denatured or unfolded proteins have a different refractive index, and this may be the reason for the whitening effect. The decrease of pH in normal cells may not be enough to cause the proteins to unfold and perhaps this is the reason that in normal tissue no variation in the IBSL is detected. Thus, the back-scattered light is strongly related to the pH dynamics influenced by the acetic acid penetration in the cervical epithelium. Nevertheless, the proteins that contribute to the effect are not well established. Moreover, each of these proteins may denature at a different pH value.

[0089] According to the other interpretation, the action of acetic acid on the epithelium of the transformation zone is related to its concentration [MacLean AB. (2004) Gynecologic Oncology, 95: 691-694]. Acetic acid enters in the cellular environment of the dysplastic layers altering the structure of different nucleoproteins and hence causing the cells to appear opaque. Thus, the dynamics of the back-scattered light follows the dynamics of the acetic acid concentration. In normal tissue, no whitening occurs because the quantity of nucleoprotein is very small.

[0090] Based on the above mentioned analysis of the functional and structural features of the epithelium undergoing changes during neoplasia development it is possible to correlate dynamic optical data with epithelial features of diagnostic importance. In particular, the measured dynamic characteristics can be used to decouple various epithelial structural and transport phenomena occurring in time sequence after the application of the biomarker, and to correlate them with *in vivo* measurable optical parameters thus providing a solution to the inverse problem. In other words, it is possible to obtain information for various epithelial features by measuring *in vivo* dynamic characteristics and parameters.

[0091] 'SlopeA' may be used to obtain information for the extracellular acidity, and in turn for the passive diffusion constant, and for the number of cell layers of the stratified epithelium. In another embodiment of the method, 'Max' is used to determine the NCR of the epithelium since the intensity of the back-scattered light is proportional to the density of signal sources (cell nuclei). 'SlopeB' may be used to obtain information in regard to the cell malfunction in regulating the intracellular pH, and to the existence of disorganized vasculature, or to the poor lymphatic drainage associated with neoplasia development. In another embodiment, the 'Integral' parameter is used to obtain combined information for both

functional and structural features as described above.

[0092] Clinical validation of this biophysical model has been performed by correlating NCR with the 'Max' and 'Integral' parameters described previously. However, clinical validation of the functional features is clinically impracticable due to the lack of reference methods capable of measuring these features *in vivo*. In contrast, the method disclosed herein is capable of modelling and predicting *in vivo* functional features of the tissue, based on its inherent capability of recording, analysing, and displaying dynamic optical characteristics obtained *in vivo* from a tissue interacting with a biomarker.

[0093] **FIG. 12** depicts a computing device 1070 which executes instructions embodied on a computer readable medium defining at least the steps illustrated in image processing engine **1085** and in conjunction with a hardware set-up utilized to obtain the tissue image data. In particular, the tissue **1020,** is constantly illuminated with a light source **1010.** After application of a suitable biomarker by means of an applicator **1030,** a trigger signal is provided to initiate image acquisition using an image acquisition device **1040** such as a video CCD or other suitable image acquisition device. Between the tissue **1020** and the image acquisition device **1040** are optical filter **1050** and lenses **1060,** for example, one or more zoomable lenses can be interposed. The optical filter **1050** can be tuned to a preferred spectral band, at which maximum contrast is obtained between areas that are subjected to different grade of alterations in their optical reflectance or fluorescence characteristics after administering an appropriate agent.

[0094] Before agent administration a tissue image is obtained as a reference. After agent administration, a series of images **1080,** in time succession, at predetermined spectral bands, and for a predetermined time period, is obtained and stored in memory or a storage device internal to or external to the computing device 1070, for further processing by the image processing engine **1085.** After proper alignment of some or all of the acquired images, a DOC **1090** is generated for a specific image location corresponding to the same tissue point. In step **1100,** a number of dynamic optical parameters expressing the dynamic characteristics of the phenomenon are derived from the DOCs, **1100.**

[0095] After extracting the DOPs, in step **1110** their values can be compared with predetermined cut-off values to, in turn, in step **1120,** classify various pathological conditions of the tissue. As one result, a pseudolor map **1130,** can then be displayed on a display device **1140,** with different colors, or grey-shades, representing different pathologies. Alternatively, the classification of the various pathological conditions of the tissue can be stored for display at another time or sent to another computing device by, for example, a packet or other unit suitable for use in transporting data in a network environment.

[0096] Alternatively, in step **1150,** the DOP values can be converted using predetermined mathematical formulas, to express functional and structural features of the tissue. In this case, a pseudolor map **1130,** can be displayed on the display device **1140** with different colors, or grey-shades, representing different functional and structural features.

Claims

1. A computer readable medium holding computer program instructions for determining structural and functional characteristics of a tissue, which when executed by a computing device causes the computing device to perform the steps of:

   calculating from an optical property of a tissue, or portion thereof that has been exposed to a biomarker over time, a dynamic optical curve,
   determining at least one dynamic optical parameter from the dynamic optical curve, wherein the at least one dynamic optical parameter is "Integral" or "Max";
   comparing the value of the at least one dynamic optical parameter with at least one reference value of the at least one dynamic optical parameter known to be linked to a structural or functional characteristic of the tissue; and
   based on the comparison, providing an output regarding a structural or functional characteristic of the tissue, or portion thereof, **characterized in that** the structural or functional characteristic of the tissue is nuclear-to-cytoplasmic-ratio of the cells of the tissue.

2. The computer readable medium of claim 1 wherein the tissue is a cervical tissue, a cervical epithelial tissue and/or comprises epithelial cells.

3. The computer readable medium of claim 1 or 2 wherein said biomarker is an acetic acid solution, preferably a 3-5% acetic acid solution.

4. The computer readable medium of any of claims 1 to 3 wherein the structural or functional characteristic of the tissue is the nuclear-to-cytoplasmic-ratio (NCR) of the cells of the tissue, where the NCR is preferably correlated

with the 'Integral' and 'Max' parameters using the formulae: $NCR = \frac{1}{1349} \times Integral - 0.278$ and

$$NCR = \frac{1}{181} \times Max - 0.309$$

5. The computer readable medium of any of claims 1 to 4 which is useful four diagnosing and/or characterizing a neoplasia.

6. The computer readable medium of any of claims 1 to 5 wherein said reference value of said dynamic optical parameter is determined by performing the steps of:

calculating a first dynamic optical curve over a period of time based on an optical property of a first tissue, or portion thereof, that has been exposed to a biomarker, wherein the first tissue is known to have a particular structural or functional characteristic;
calculating a second dynamic optical curve over a period of time based on an optical property of a second tissue, or portion thereof, that has been exposed to a biomarker, wherein the second tissue is known to not have a particular structural or functional characteristic;
based on said first dynamic optical curve, determining a first value of at least one dynamic optical parameter and based on said second dynamic optical curve, determining a second value of at least one dynamic optical parameter; and
by a comparison of said first value and said second value, correlating the at least one dynamic optical parameter with a particular structural or functional characteristic of a tissue.

7. The computer readable medium of claim 6 wherein the steps for calculating a first dynamic optical curve and determining said first value are repeated a number of times using a separate tissue sample known to have a particular structural or functional characteristic each time resulting in a group of first values;
wherein the steps for calculating a second dynamic optical curve and determining said second value are repeated a number of times using a separate tissue sample known not to have a particular structural or functional characteristic each time resulting in a group of second values, and
wherein the step of correlating the at least one dynamic optical parameter and said particular structural or functional characteristic includes comparing the group of first values and the group of second values to determine a reference value of said at least one dynamic optical parameter.

8. The computer readable medium of any of claims 1 to 7, wherein a plurality of the at least one dynamic optical parameters are used for determining structural and functional characteristics of a tissue, or portion thereof via a combination of the plurality of dynamic optical parameters with the aid of an Artificial Neural Network, statistical pattern recognition algorithm, Bayesian classification, or classification trees.

9. The computer readable medium of any of claims 1 to 8, wherein the determined dynamic optical curve/at least one dynamic optical parameter/structural or functional characteristic of the tissue, or portion thereof is represented by a particular colour on a pseudocolour map of the tissue or portion thereof.

10. The computer readable medium of any of claims 1 to 9, wherein said dynamic optical curve represents the temporal variation of the diffuse reflectance obtained from a tissue site.

11. An automated and quantitative method for determining structural and functional characteristics of a tissue, comprising use of a computer readable medium as defined in any of claims 1 to 10 wherein the tissue, or portion thereof, has been exposed to topical application of a biomarker.

12. The method of claim 11, wherein a reference image of the tissue is acquired prior to application of a biomarker.

13. The method of claim 11 or 12, wherein a dynamic optical curve is calculated at every image pixel corresponding to

a single point on the tissue.

14. The method of any of claims 11 to 13, wherein the generation of data for a dynamic optical curve comprises aligning captured images of the tissue, or portion thereof.

Patentansprüche

1. Computerlesbares Medium, welches Computerprogrammanweisungen zum Bestimmen von strukturellen und funktionalen Merkmalen eines Gewebes umfasst, welche bei Ausführung durch eine Computervorrichtung die Computervorrichtung veranlassen, die Schritte auszuführen:

Berechnen einer dynamischen optischen Kurve aus einer optischen Eigenschaft eines Gewebes oder eines Abschnitts desselben, welches/welcher über eine Zeit einem Biomarker ausgesetzt wurde;
Bestimmen von wenigstens einem dynamischen optischen Parameter aus der dynamischen optischen Kurve, wobei der wenigstens eine dynamische optische Parameter "Integral" oder "Max" ist;
Vergleichen des Wertes des wenigstens einen dynamischen optischen Parameters mit wenigstens einem Referenzwert des wenigstens einen dynamischen optischen Parameters, der bekannterweise mit einem strukturellen oder funktionalen Merkmal des Gewebes zusammenhängt; und
Bereitstellen, auf Grundlage des Vergleichs, einer Ausgabe bezüglich eines strukturellen oder funktionalen Merkmals des Gewebes oder Abschnitts desselben,
dadurch gekennzeichnet,
dass das strukturelle oder funktionale Merkmal des Gewebes ein Nukleus-zu-Cytoplasma-Verhältnis der Zellen des Gewebes ist.

2. Computerlesbares Medium nach Anspruch 1,
wobei das Gewebe ein zervikales Gewebe ist, ein zervikales Epithelgewebe ist oder/und Epithelzellen umfasst.

3. Computerlesbares Medium nach Anspruch 1 oder 2,
wobei der Biomarker eine Essigsäurelösung, vorzugsweise eine 3-5% Essigsäurelösung ist.

4. Computerlesbares Medium nach einem der Ansprüche 1 bis 3,
wobei das strukturelle oder funktionale Merkmal des Gewebes das Nukleus-zu-Cytoplasma-Verhälthis (NCR) der Zellen des Gewebes ist, wobei das NCR vorzugsweise mit den Parametern "Integral" oder "Max" unter Verwendung der Formeln

$$NCR = \frac{1}{1349} \times Integral - 0.278$$

und

$$NCR = \frac{1}{181} \times Max - 0.309$$

korreliert ist.

5. Computerlesbares Medium nach einem der Ansprüche 1 bis 4, welches zur Diagnose oder/und Kennzeichnung von Neoplasmen hilfreich ist.

6. Computerlesbares Medium nach einem der Ansprüche 1 bis 5,
wobei der Referenzwert des dynamischen optischen Parameters bestimmt wird, durch Ausführen der Schritte:

Berechnen einer ersten dynamischen optischen Kurve über einen Zeitraum auf Grundlage einer optischen Eigenschaft eines ersten Gewebes oder eines Abschnitts desselben, welches/welcher einem Biomarker ausgesetzt wurde, wobei das erste Gewebe bekannterweise ein bestimmes strukturelles oder funktionales Merkmal aufweist;

Berechnen einer zweiten dynamischen optischen Kurve über einen Zeitraum auf Grundlage einer optischen Eigenschaft eines zweiten Gewebes oder eines Abschnitts desselben, welches/welcher einem Biomarker ausgesetzt wurde, wobei das zweite Gewebe bekannterweise ein bestimmtes strukturelles oder funktionales Merkmal nicht aufweist;

Bestimmen eines ersten Wertes von wenigstens einem dynamischen optischen Parameter auf Grundlage der ersten dynamischen optischen Kurve und Bestimmen eines zweiten Wertes von wenigstens einem dynamischen optischen Parameter auf Grundlage der zweiten dynamischen optischen Kurve; und

Korrelieren des wenigstens einen dynamischen optischen Parameters mit einem bestimmten strukturellen oder funktionalen Merkmal eines Gewebes, durch einen Vergleich des ersten Wertes mit dem zweiten Wert.

7. Computerlesbares Medium nach Anspruch 6,
wobei die Schritte zum Berechnen einer ersten dynamischen optischen Kurve und zum Bestimmen des ersten Wertes eine Anzahl von Malen wiederholt werden, wobei jedes Mal eine gesonderte Gewebeprobe verwendet wird, die bekannterweise ein bestimmtes strukturelles oder funktionales Merkmal aufweist, wobei eine Gruppe von ersten Werten erhalten wird;
wobei die Schritte zum Berechnen einer zweiten dynamischen optischen Kurve und zum Bestimmen des zweiten Wertes eine Anzahl von Malen wiederholt werden, wobei jedes Mal eine gesonderte Gewebeprobe verwendet wird, die bekannterweise ein bestimmtes strukturelles oder funktionales Merkmal nicht aufweist, wobei eine Gruppe von zweiten Werten erhalten wird; und
wobei der Schritt des Korrelierens des wenigstens einen dynamischen optischen Parameters und des bestimmten strukturellen oder funktionalen Merkmals einen Vergleich der Gruppe von ersten Werten und der Gruppe von zweiten Werten umfasst, um einen Referenzwert des wenigstens einen dynamischen optischen Parameters zu bestimmen.

8. Computerlesbares Medium nach einem der Ansprüche 1 bis 7,
wobei eine Mehrzahl von dem wenigstens einen dynamischen optischen Parameter zum Bestimmen von strukturellen und funktionalen Merkmalen eines Gewebes oder eines Abschnitts desselben verwendet werden, durch eine Kombination der Mehrzahl von dynamischen optischen Parametern mithilfe eines künstlichen neuronalen Netzwerks, eines statistischen Mustererkennungsalgorithmus, einer bayesianischen Klassifikation oder von Klassifikationsbäumen.

9. Computerlesbares Medium nach einem der Ansprüche 1 bis 8,
wobei die bestimmte dynamische optische Kurve/der wenigstens eine dynamische optische Parameter/das strukturelle oder funktionale Merkmal des Gewebes oder Abschnitts desselben durch eine bestimmte Farbe auf einer Pseudofarbkarte des Gewebes oder Abschnitts desselben dargestellt ist.

10. Computerlesbares Medium nach einem der Ansprüche 1 bis 9,
wobei die dynamische optische Kurve die zeitliche Variation der von einer Gewebestelle erhaltenen diffusen Reflektion darstellt.

11. Automatisiertes und quantitatives Verfahren zum Bestimmen von strukturellen und funktionalen Merkmalen eines Gewebes, umfassend ein Verwenden eines computerlesbaren Mediums nach einem der Ansprüche 1 bis 10,
wobei das Gewebe oder der Abschnitt desselben einer örtlichen Anwendung eines Biomarkers ausgesetzt wurde.

12. Verfahren nach Anspruch 11, wobei ein Referenzbild des Gewebes vor einer Anwendung eines Biomarkers erfasst wird.

13. Verfahren nach Anspruch 11 oder 12,
wobei eine dynamische optische Kurve an jedem Bildpixel berechnet wird, welches einem einzelnen Punkt auf dem Gewebe entspricht.

14. Verfahren nach einem der Ansprüche 11 bis 13,
wobei das Erzeugen von Daten für eine dynamische optische Kurve, ein Ausrichten von aufgenommenen Bildern des Gewebes oder Abschnitts desselben umfasst.

Revendications

1. Support lisible par ordinateur contenant des instructions de programme informatique pour déterminer les caracté-

ristiques fonctionnelles et structurales d'un tissu, qui, lorsqu'elles sont exécutées par un dispositif informatique amènent le dispositif informatique à exécuter les étapes qui consistent:

à calculer une courbe optique dynamique d'après une propriété optique d'un tissu, ou d'une partie de celui-ci qui a été exposée au cours du temps à un marqueur biologique,
à déterminer au moins un paramètre optique dynamique d'après la courbe optique dynamique, où l'au moins un paramètre optique dynamique est "Intégral" ou "Maximal" ;
à comparer la valeur de l'au moins un paramètre optique dynamique à au moins une valeur de référence de l'au moins un paramètre optique dynamique connu pour être rattaché à une caractéristique structurale ou fonctionnelle du tissu ; et
à fournir, sur la base de la comparaison, une sortie concernant une caractéristique structurale ou fonctionnelle du tissu, ou d'une partie de celui-ci, **caractérisé en ce que** la caractéristique structurale ou fonctionnelle du tissu est un rapport nucléo-cytoplasmique des cellules du tissu.

2. Support lisible par ordinateur de la revendication 1 dans lequel le tissu est un tissu cervical, un tissu épithélial cervical et/ou comprend des cellules épithéliales.

3. Support lisible par ordinateur de la revendication 1 ou 2 dans lequel ledit marqueur biologique est une solution d'acide acétique, de préférence une solution d'acide acétique à 3 à 5%.

4. Support lisible par ordinateur de l'une des revendications 1 à 3 dans lequel la caractéristique structurale ou fonctionnelle du tissu est le rapport nucléo-cytoplasmique (NCR) des cellules du tissu, où le NCR est de préférence corrélé aux paramètres "Intégral" et "Maximal" en utilisant les formules :

$$NCR = \frac{1}{1349} \times Intégral - 0,278$$

et

$$NCR = \frac{1}{181} \times Max - 0,309$$

5. Support lisible par ordinateur de l'une des revendications 1 à 4 qui sert à diagnostiquer et/ou à caractériser une néoplasie.

6. Support lisible par ordinateur de l'une des revendications 1 à 5 dans lequel ladite valeur de référence dudit paramètre optique dynamique est déterminée en exécutant les étapes qui consistent:

à calculer une première courbe optique dynamique pendant une durée sur la base d'une propriété optique d'un premier tissu, ou d'une partie de celui-ci, qui a été exposé à un marqueur biologique, où le premier tissu est connu pour avoir une caractéristique structurale ou fonctionnelle particulière;
à calculer pendant une durée une deuxième courbe optique dynamique sur la base d'une propriété optique d'un deuxième tissu, ou d'une partie de celui-ci, qui a été exposé à un marqueur biologique; où le deuxième tissu est connu pour avoir une caractéristique structurale ou fonctionnelle particulière;
à déterminer, sur la base de ladite première courbe optique, une première valeur d'au moins un paramètre optique dynamique et à déterminer, sur la base de ladite deuxième courbe dynamique, une deuxième valeur d'au moins un paramètre optique dynamique; et
à corréler, par comparaison de ladite première valeur et de ladite deuxième valeur, l'au moins un paramètre optique dynamique à une caractéristique structurale ou fonctionnelle particulière d'un tissu.

7. Support lisible par ordinateur de la revendication 6 dans lequel les étapes qui consistent à calculer une courbe optique dynamique et à déterminer ladite première valeur sont répétées un nombre de fois en utilisant un échantillon de tissu séparé connu pour avoir une caractéristique structurale ou fonctionnelle particulière résultant à chaque fois en un groupe de premières valeurs ;
où les étapes destinées à calculer une deuxième courbe optique dynamique et à déterminer ladite deuxième valeur sont répétées un nombre de fois en utilisant un échantillon de tissu séparé connu pour ne pas avoir de caractéristique

structurale ou fonctionnelle particulière résultant à chaque fois en un groupe de deuxièmes valeurs; et
où l'étape qui consiste à corréler l'au moins un paramètre optique dynamique et ladite caractéristique structurale ou fonctionnelle particulière comporte le fait de comparer le groupe de premières valeurs et le groupe de deuxièmes valeurs afin de déterminer une valeur de référence dudit au moins un paramètre optique dynamique.

8. Support lisible par ordinateur de l'une des revendications 1 à 7, dans lequel une pluralité de l'au moins un paramètre optique dynamique sont utilisés pour déterminer les caractéristiques structurales et fonctionnelles d'un tissu, ou une partie de celui-ci au moyen d'une combinaison de la pluralité de paramètres optiques dynamiques à l'aide d'un Réseau de Neurones Artificiels, d'un algorithme de reconnaissance de modèles statistiques, d'une classification Bayésienne, ou d'arbres de classification.

9. Support lisible par ordinateur de l'une des revendications 1 à 8, dans lequel la courbe optique dynamique déterminée/l'au moins un paramètre optique dynamique/la caractéristique structurale ou fonctionnelle du tissu, ou une partie de celui-ci est représenté par une couleur particulière sur une carte de pseudo-couleurs du tissu ou d'une partie de celui-ci.

10. Support lisible par ordinateur de l'une des revendications 1 à 9, dans lequel ladite courbe optique dynamique représente la variation temporelle de la réflectance diffuse obtenue à partir d'un emplacement de tissu.

11. Procédé quantitatif et automatisé visant à déterminer les caractéristiques structurales et fonctionnelles d'un tissu, comprenant l'utilisation d'un support lisible par ordinateur tel que défini dans l'une des revendications 1 à 10 où le tissu, ou une partie de celui-ci, a été exposé à une application topique d'un marqueur biologique.

12. Procédé de la revendication 11, dans lequel une image de référence du tissu est acquise avant l'application d'un marqueur biologique.

13. Procédé de la revendication 11 ou 12, dans lequel une courbe optique dynamique est calculée à chaque pixel d'image correspondant à un seul point sur le tissu.

14. Procédé de l'une des revendications 11 à 13, dans lequel la génération de données pour une courbe optique dynamique comprend le fait d'aligner des images capturées du tissu, ou d'une partie de celui-ci.

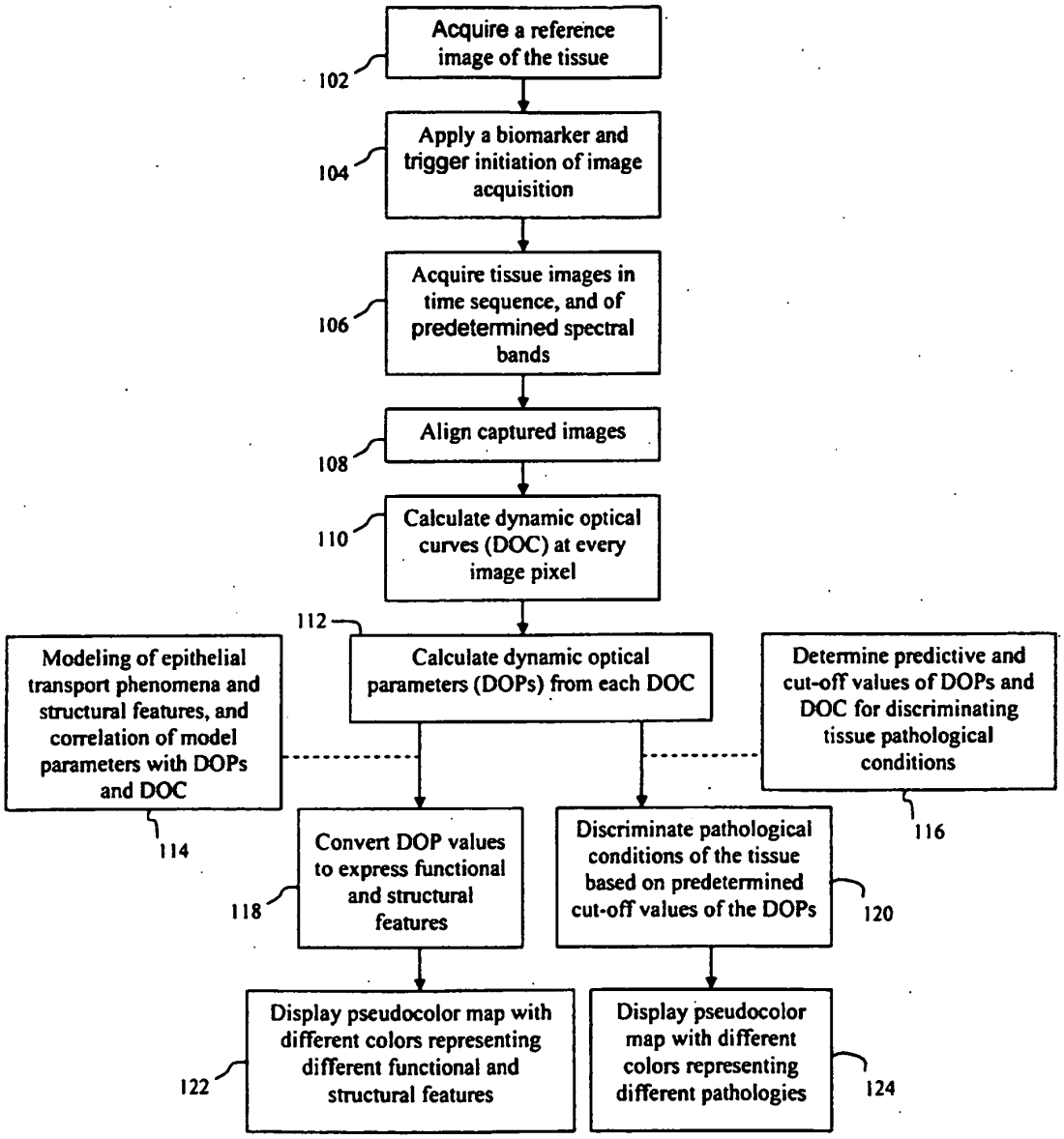
Acquire a reference image of the tissue
102
Apply a biomarker and trigger initiation of image acquisition
104
Acquire tissue images in time sequence, and of predetermined spectral bands
106
Align captured images
108
Calculate dynamic optical curves (DOC) at every image pixel
110
112
Calculate dynamic optical parameters (DOPs) from each DOC
Modeling of epithelial transport phenomena and structural features, and correlation of model parameters with DOPs and DOC
114
Determine predictive and cut-off values of DOPs and DOC for discriminating tissue pathological conditions
116
Convert DOP values to express functional and structural features
118
Discriminate pathological conditions of the tissue based on predetermined cut-off values of the DOPs
120
Display pseudocolor map with different colors representing different functional and structural features
122
Display pseudocolor map with different colors representing different pathologies
124

FIG. 1

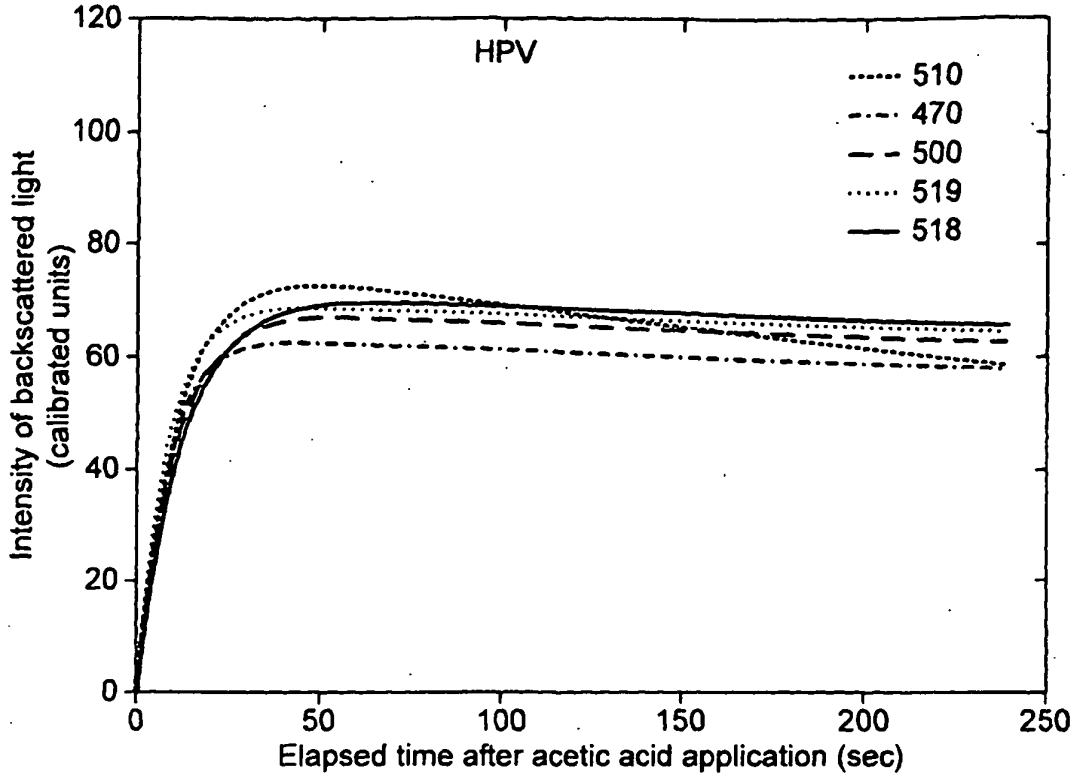
HPV
510
470
500
519
518
Intensity of backscattered light (calibrated units)
Elapsed time after acetic acid application (sec)
0
20
40
60
80
100
120
0
50
100
150
200
250

FIG. 2

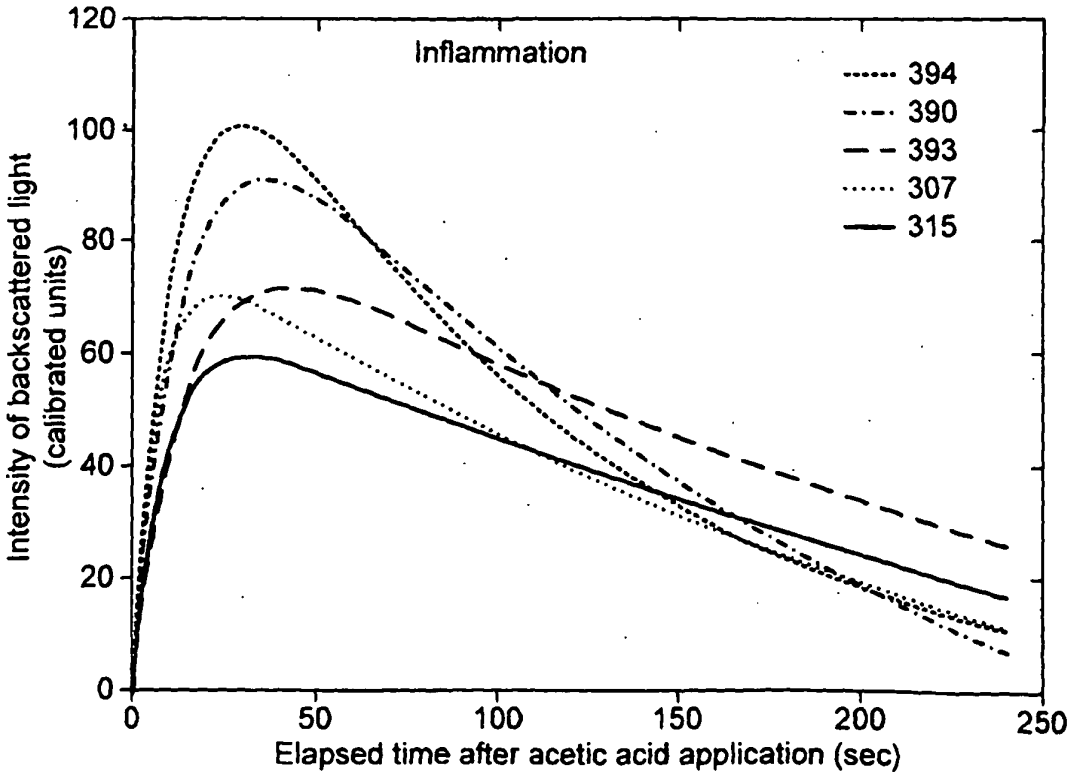
Inflammation
394
390
393
307
315
Intensity of backscattered light (calibrated units)
Elapsed time after acetic acid application (sec)
0
20
40
60
80
100
120
0
50
100
150
200
250

FIG. 3

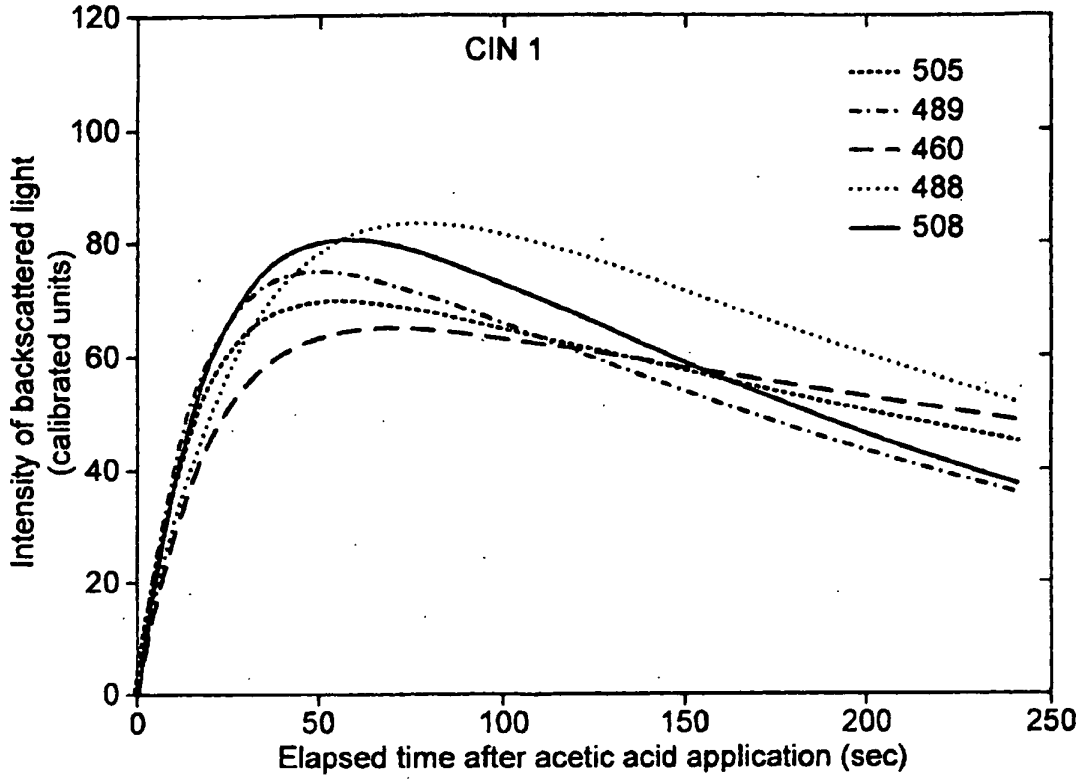
CIN 1
505
489
460
488
508
Intensity of backscattered light (calibrated units)
Elapsed time after acetic acid application (sec)
0
20
40
60
80
100
120
0
50
100
150
200
250

FIG. 4

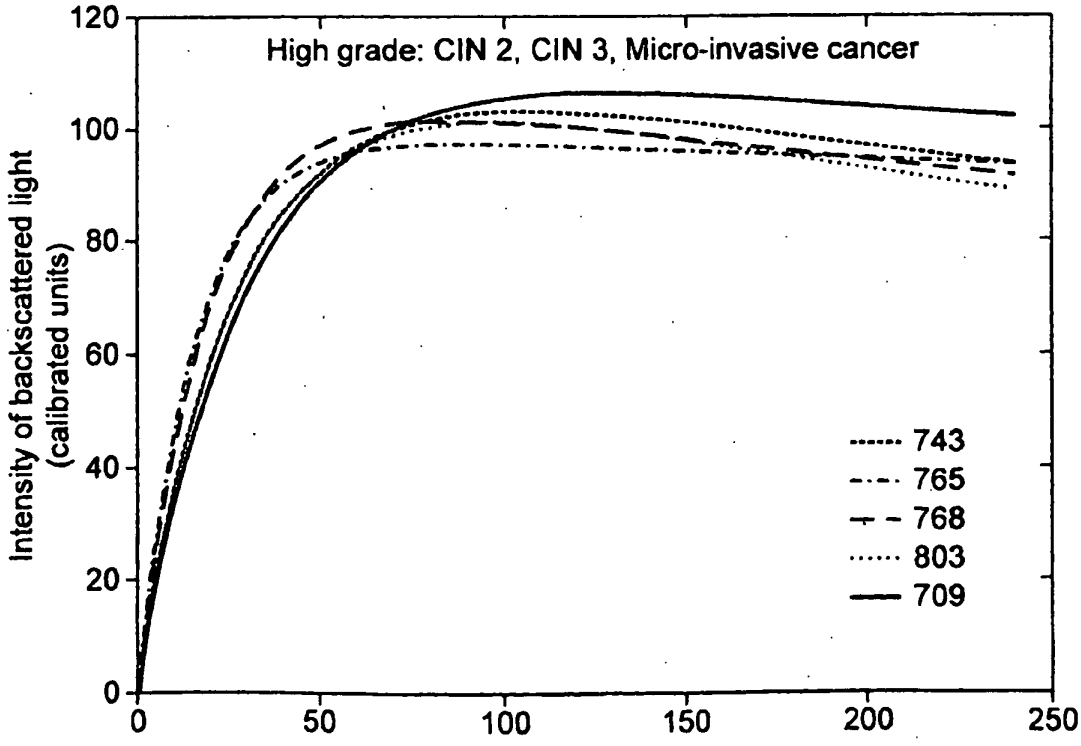
High grade: CIN 2, CIN 3, Micro-invasive cancer
743
765
768
803
709
Intensity of backscattered light (calibrated units)
0
20
40
60
80
100
120
0
50
100
150
200
250

FIG. 5

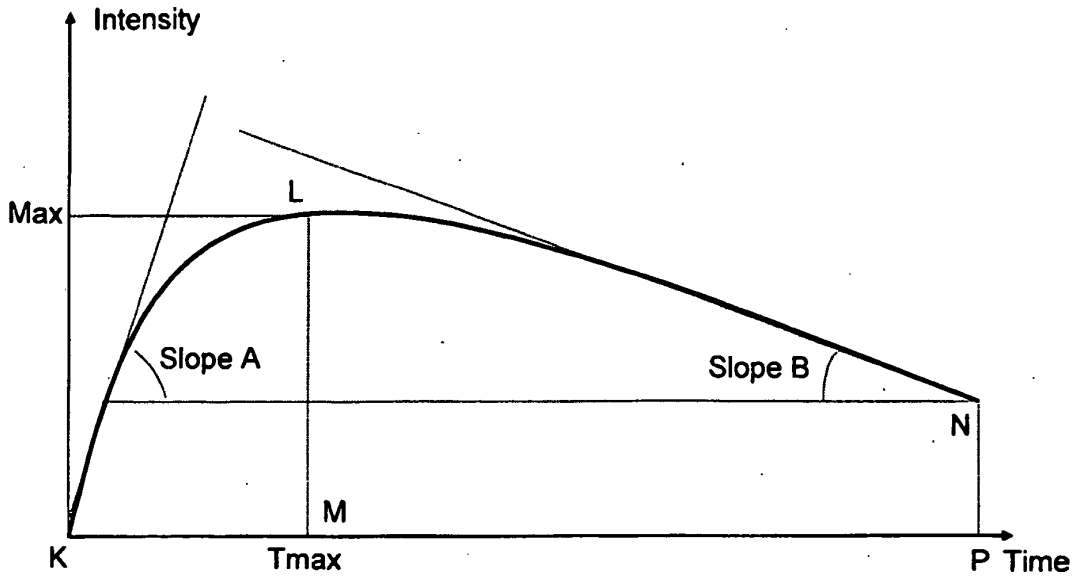
Intensity
Max
L
Slope A
Slope B
N
M
K
Tmax
P Time

FIG. 6

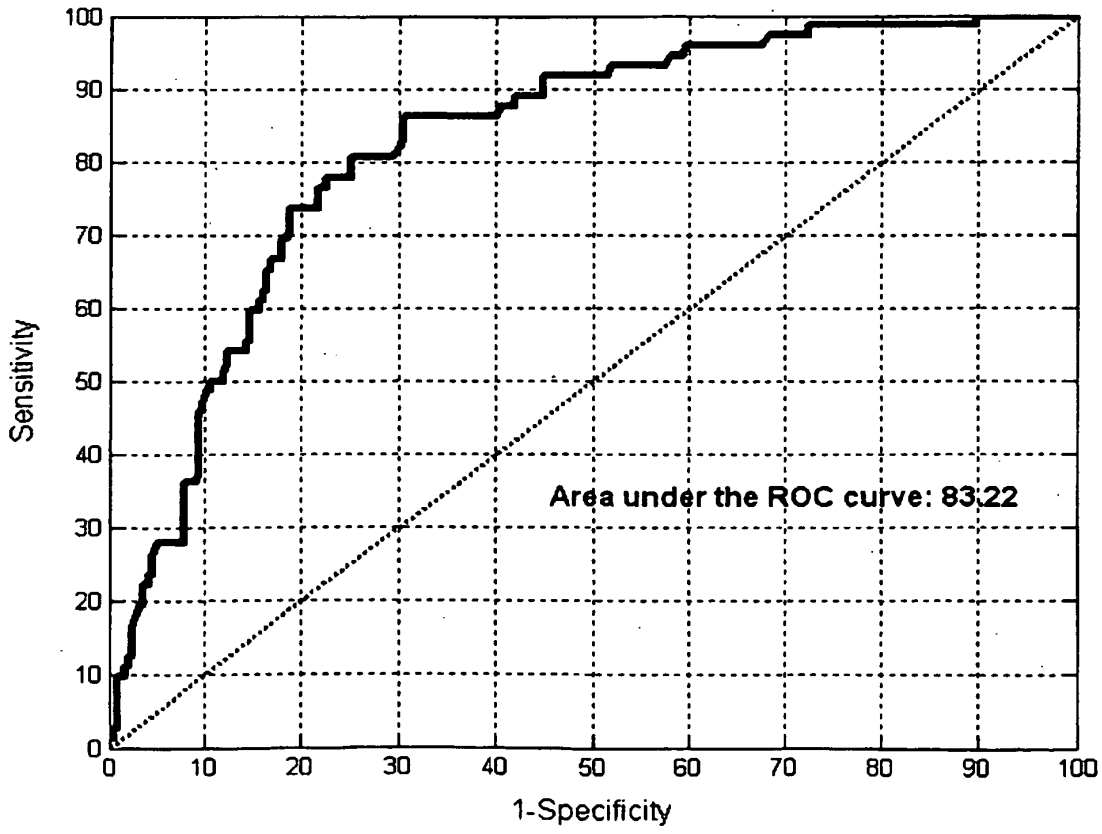
Sensitivity
1-Specificity
Area under the ROC curve: 83.22
0
10
20
30
40
50
60
70
80
90
100

FIG. 7

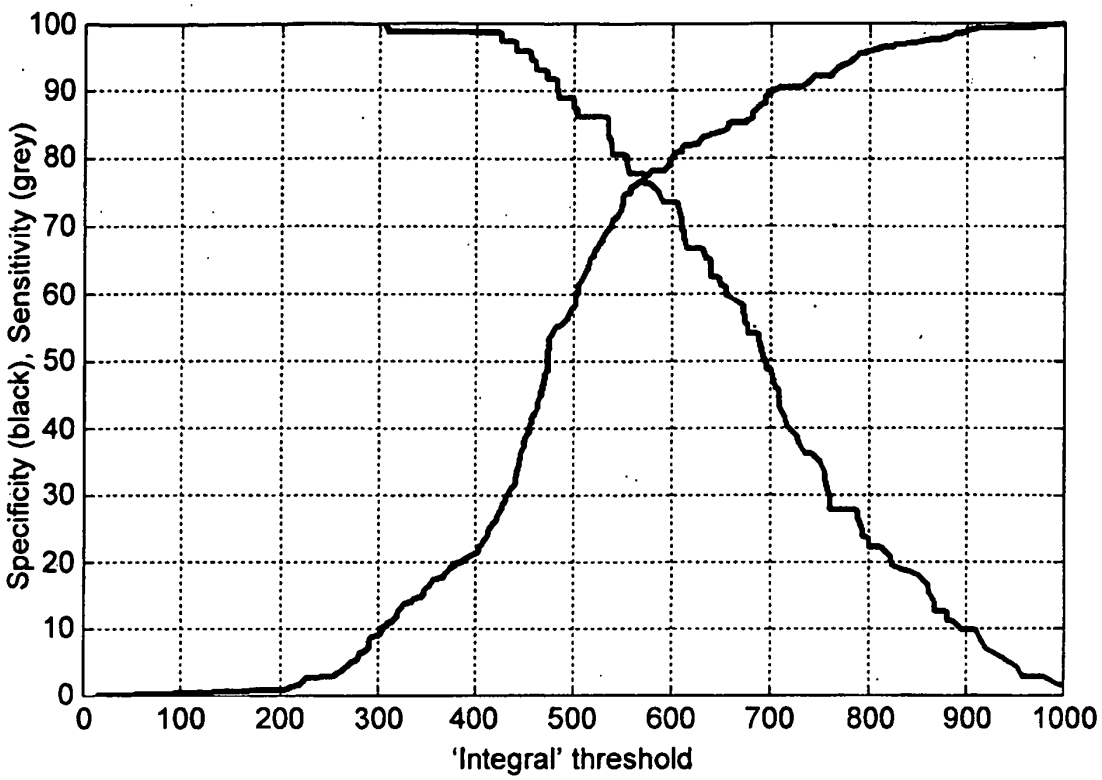
Specificity (black), Sensitivity (grey)
'Integral' threshold
0
10
20
30
40
50
60
70
80
90
100
0
100
200
300
400
500
600
700
800
900
1000

FIG. 8

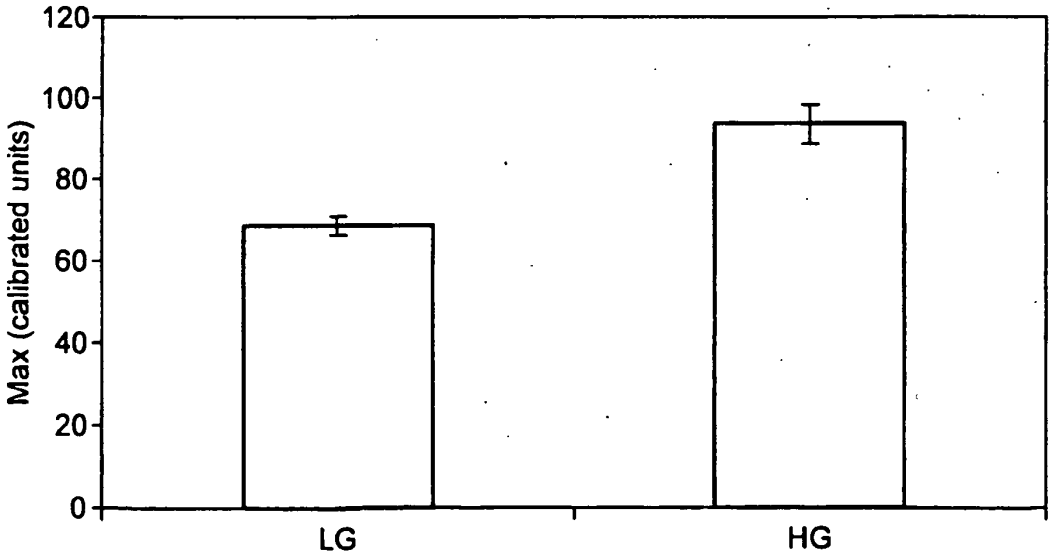
Max (calibrated units)
0
20
40
60
80
100
120
LG
HG

FIG. 9A

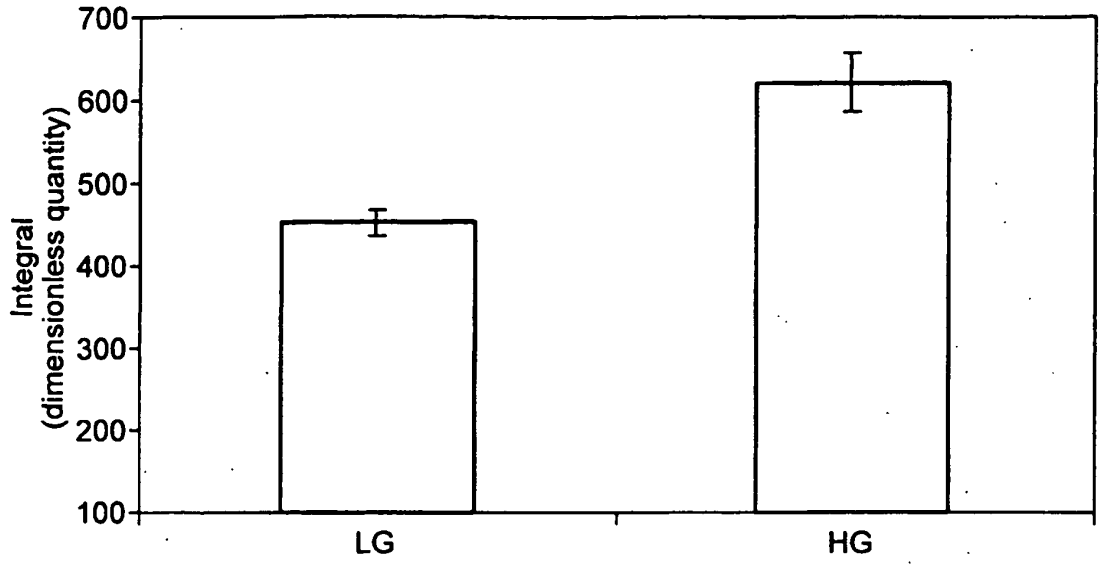
700
600
500
400
300
200
100
Integral
(dimensionless quantity)
LG
HG

FIG. 9B

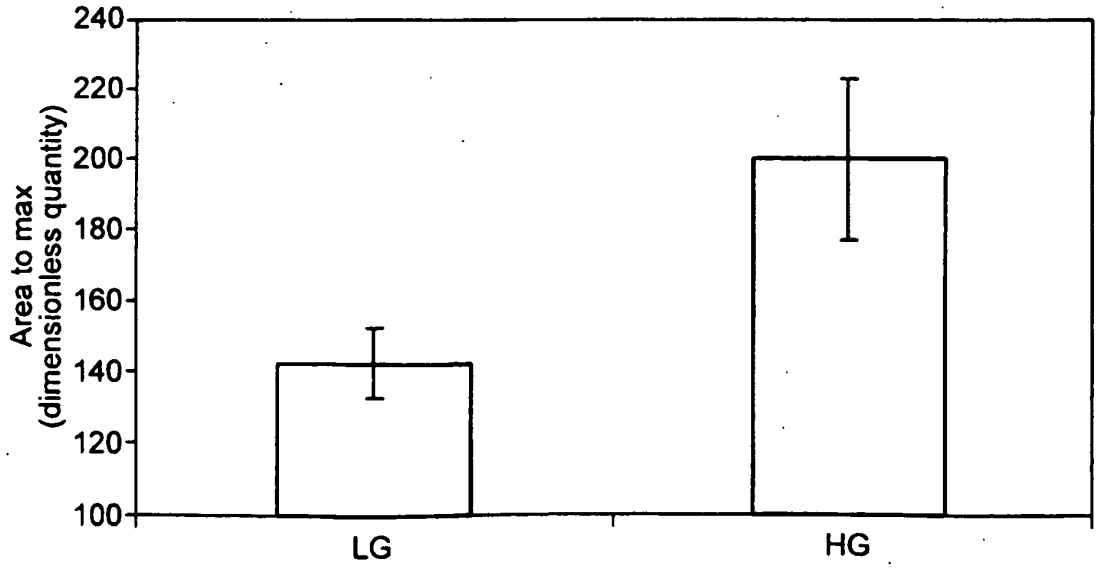
240
220
200
180
160
140
120
100
Area to max
(dimensionless quantity)
LG
HG

FIG. 9C

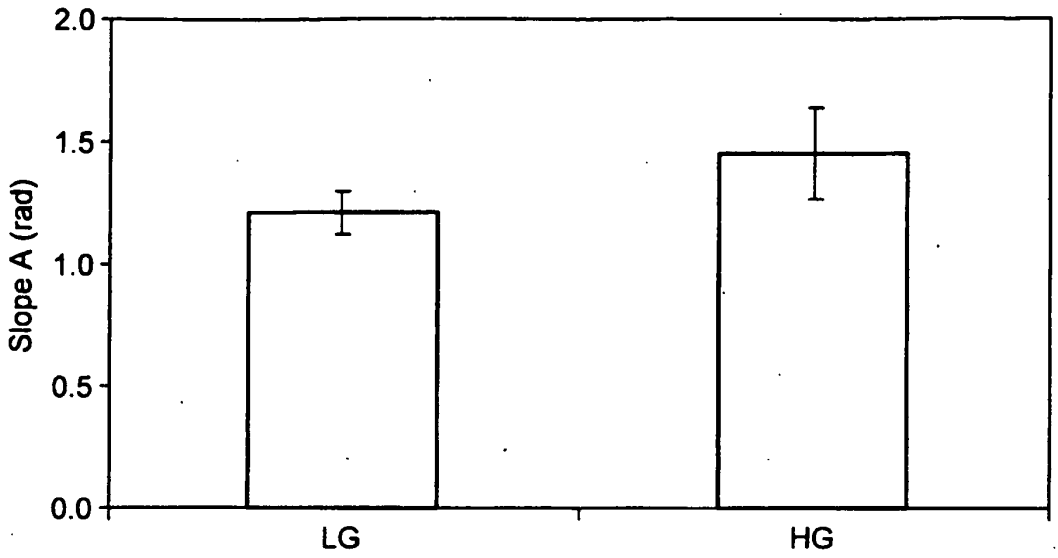
2.0
1.5
1.0
0.5
0.0
Slope A (rad)
LG
HG

FIG. 9D

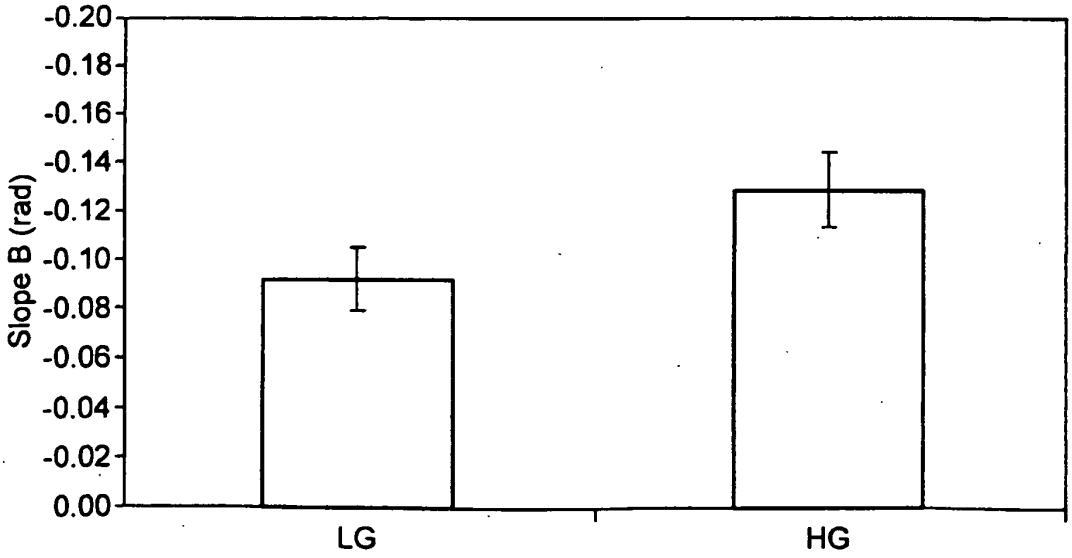
-0.20
-0.18
-0.16
-0.14
-0.12
-0.10
-0.08
-0.06
-0.04
-0.02
0.00
Slope B (rad)
LG
HG

FIG. 9E

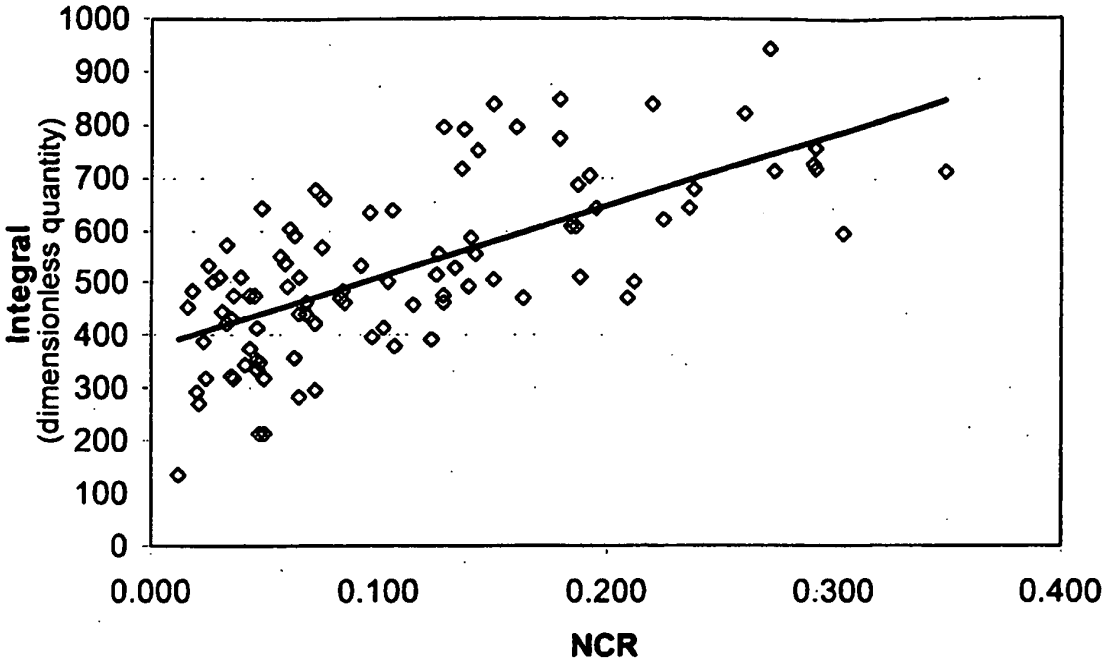

FIG. 10A

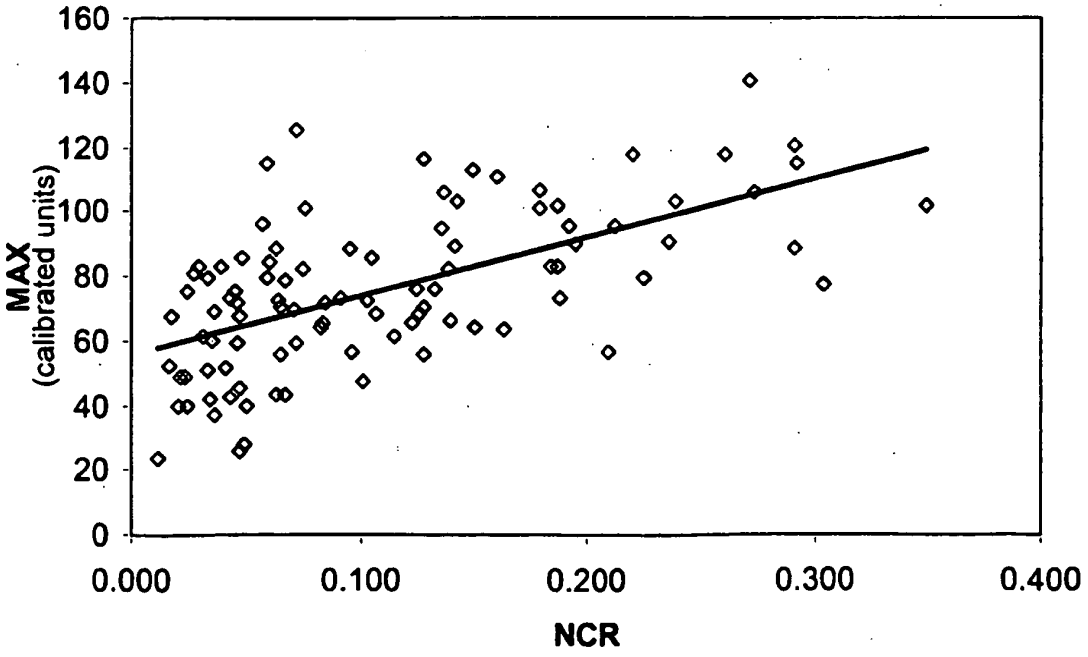

FIG. 10B

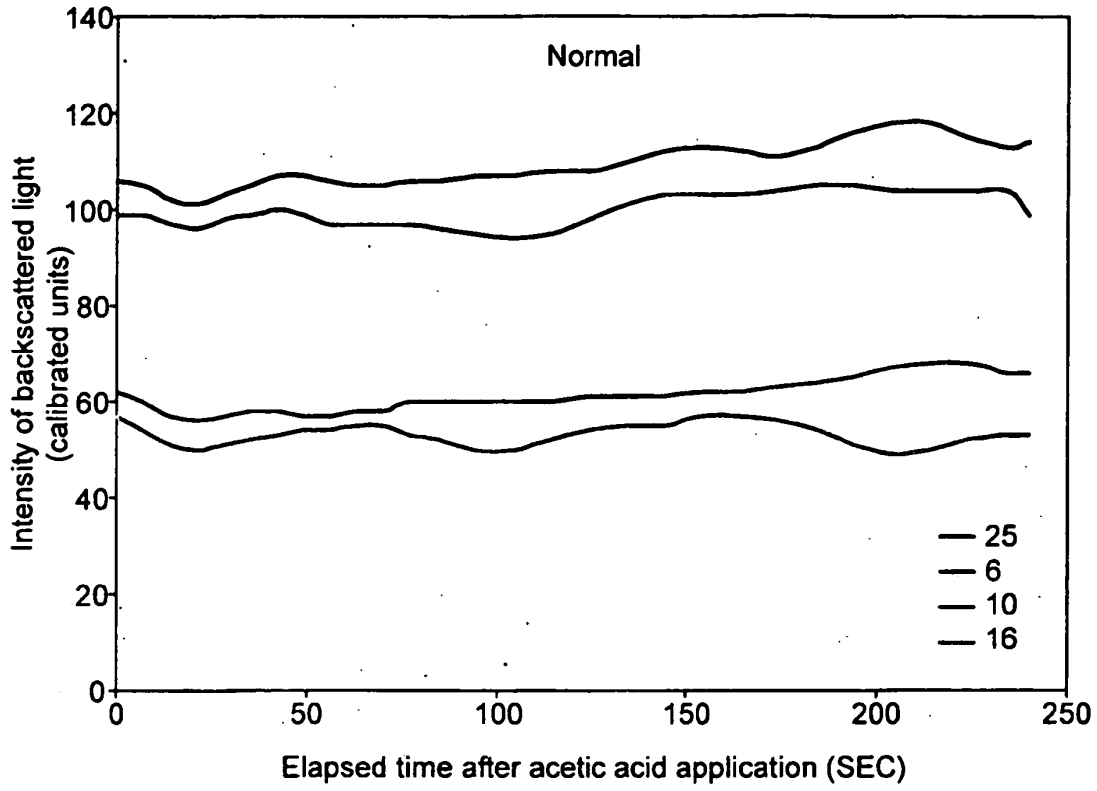
Normal
Intensity of backscattered light (calibrated units)
140
120
100
80
60
40
20
0
0
50
100
150
200
250
Elapsed time after acetic acid application (SEC)
25
6
10
16

FIG. 11

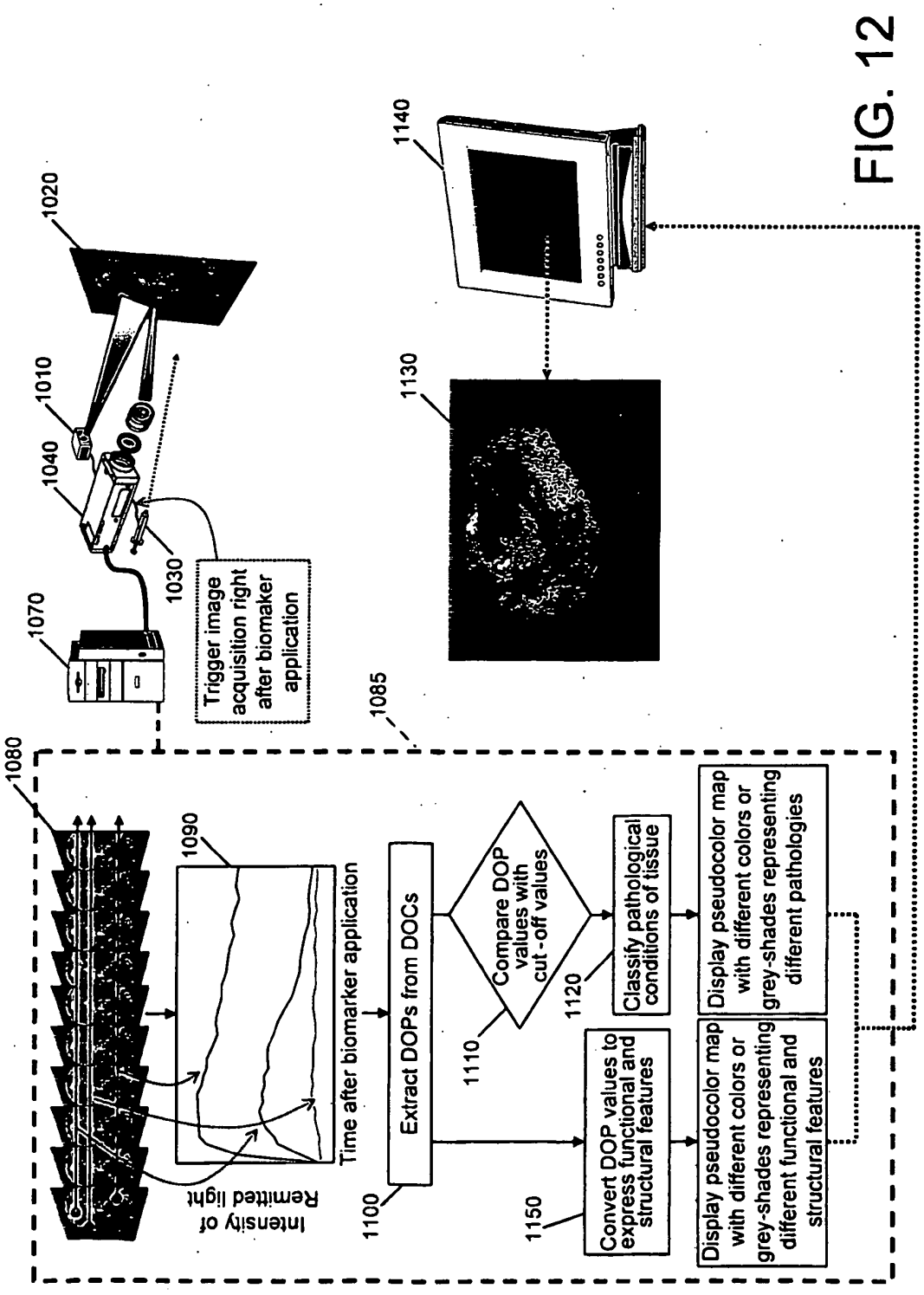
1020
1010
1040
1030
1070
Trigger image acquisition right after biomaker application
1140
1130
1085
1080
1090
Intensity of Remitted light
Time after biomarker application
Extract DOPs from DOCs
1100
Compare DOP values with cut-off values
1110
Classify pathological conditions of tissue
1120
Display pseudocolor map with different colors or grey-shades representing different pathologies
Convert DOP values to express functional and structural features
1150
Display pseudocolor map with different colors or grey-shades representing different functional and structural features

FIG. 12

REFERENCES CITED IN THE DESCRIPTION

This list of references cited by the applicant is for the reader's convenience only. It does not form part of the European patent document. Even though great care has been taken in compiling the references, errors or omissions cannot be excluded and the EPO disclaims all liability in this regard.

Patent documents cited in the description

- US 4930516 A **[0010]**
- US 5562100 A **[0011]**
- US 5467767 A **[0011]**
- US 6975899 B **[0012]**
- US 5369496 A, Utzinger **[0013]**
- US 6427082 A **[0013]**
- WO 0172214 A1 **[0015] [0022] [0033]**
- US 20020007122 A **[0018]**
- WO 2004005885 A **[0021]**

Non-patent literature cited in the description

- **Nanda K et al.** Annals of Internal Medicine. 2000, vol. 132, 810-819 **[0004]**
- **Sankaranarayanana R et al.** *International Journal of Gynecology and Obstetrics,* 2005, vol. 89, S4-S12 **[0004]**
- **Fahey MT et al.** *American Journal of Epidemiology,* 1995, vol. 141, 680-689 **[0004]**
- **Mitchell MF et al.** *Obstetrics & Gynecology,* 1998, vol. 91, 626-631 **[0006]**
- **Schiffman M et al.** *Arch. Pathol. Lab. Med.,* 2003, vol. 127, 946-949 **[0006]**
- **Cantor SB et al.** *Obstetrics & Gynecology,* 1998, vol. 91 (2), 270-277 **[0006]**
- **Ismail SM et al.** *British Medical Journal,* 1989, vol. 298 (6675), 707-710 **[0007]**
- **Bellina JH et al.** *South Med. J.,* 1982, vol. 75 (1), 6-8. 56 **[0007]**
- **Robertson AJ et al.** *J. Clin. Pathol.,* 1989, vol. 42 (3), 231-238 **[0007]**
- **Balas C.** *IEEE Trans. on Biomedical Engineering,* 2001, vol. 48, 96-104 **[0015] [0022] [0033]**
- **Balas CJ et al.** *SPIE,* 1999, vol. 3568, 31-37 **[0015] [0022] [0033]**
- **Stefanaki et al.** *Journal of Photochemistry and Photobiology B: Biology,* 2001, vol. 65, 115-121 **[0019]**
- **Orfanoudaki et al.** *Gynecologic Oncology,* 2005, vol. 96, 119-131 **[0020]**
- **DeCherney, A. et al.** Current Obstetric & Gynecologic Diagnosis & Treatment. The McGraw-Hill Companies, 2003 **[0049]**
- **Kohonen T.** *Int. J. Quant. Chem.,* 1986, vol. 13, 209-21 **[0076]**
- **Walker DC et al.** *Physiological Measurement,* 2003, vol. 24, 1-15 **[0079]**
- **Loukas CG et al.** *Cytometry,* 2003, vol. 55A (1), 30-42 **[0081]**
- **Webb SD.** *J. Theor. Biol.,* 1999, vol. 196, 237-250 **[0084] [0085]**
- **Lee AH et al.** *Cancer Research,* 1998, vol. 58, 1901-1908 **[0084] [0085]**
- **Yamagata M et al.** *Br. J. Cancer,* 1996, vol. 73, 1328-1334 **[0084] [0085]**
- **Marion S et al.** *Molecular Medicine Today,* 2000, vol. 6, 15-19 **[0084] [0085]**
- **Prescott DM et al.** *Clinical Cancer Research,* 2000, vol. 6 (6), 2501-2505 **[0085]**
- **Maddox P et al.** *Journal of Clinical Pathology,* 1999, vol. 52, 41-46 **[0087]**
- **Carrilho C et al.** *Human Pathology,* 2004, vol. 35, 546-551 **[0087]**
- **MacLean AB.** *Gynecologic Oncology,* 2004, vol. 95, 691-694 **[0089]**

专利名称(译)	表征组织的方法		
公开(公告)号	EP1978867B1	公开(公告)日	2011-05-25
申请号	EP2007823884	申请日	2007-06-05
申请(专利权)人(译)	FORTH光子有限公司		
当前申请(专利权)人(译)	FORTH PHOTONICS LIMITED		
[标]发明人	BALAS KONSTANTINOS		
发明人	BALAS, KONSTANTINOS		
IPC分类号	A61B5/00 G01N33/483 G01N33/58		
CPC分类号	G01N33/57407 A61B5/0059 A61B5/7264		
优先权	60/810930 2006-06-05 US		
其他公开文献	EP1978867A2		
外部链接	Espacenet		

摘要(译)

用于确定组织的结构和功能特征和/或病理状态的定量方法包括基于组织或其部分的光学特性在一段时间内生成动态光学曲线的数据的步骤。暴露于生物标志物，并基于该数据确定动态光学参数的值。将动态光学参数的值与已知与组织的结构或功能特征和/或病理状态相关联的动态光学参数的参考值进行比较。基于该比较，确定组织或其部分的结构或功能特征和/或病理状态。计算机可读介质保存用于执行该方法的计算机程序指令。可以通过测量来自已知代表性组织样品的动态光学性质来计算参考值。优选的组织样品包括上皮和宫颈组织样品。优选的方法包括诊断和/或分级瘤形成和/或HPV感染和/或计算组织样品中细胞的细胞核与细胞质比率。